Toxicology and Applied Pharmacology 387 (2020) 114847

Contents lists available at ScienceDirect

Toxicology and Applied Pharmacology

journal homepage: www.elsevier.com/locate/taap

Evaluation of the dose-response and fate in the lung and pleura of chrysotile-containing brake dust compared to TiO_2, chrysotile, crocidolite or amosite asbestos in a 90-day quantitative inhalation toxicology study – Interim results Part 2: Histopathological examination, Confocal microscopy and collagen quantification of the lung and pleural cavity

D.M. Bernstein[a,*], B. Toth[b], R.A. Rogers[c], D.E. Kling[c], P. Kunzendorf[d], J.I. Phillips[e], H. Ernst[f]

[a] Consultant in Toxicology, Geneva, Switzerland
[b] Citoxlab Hungary, Veszprém, Szabadságpuszta, Hungary
[c] Rogers Imaging, Natick, MA, USA
[d] GSA Gesellschaft für Schadstoffanalytik mbH, Ratingen, Germany
[e] National Institute for Occupational Health, National Health Laboratory Service, Johannesburg South Africa and Department of Biomedical Technology, Faculty of Health Sciences, University of Johannesburg, Johannesburg, South Africa
[f] Fraunhofer Institute for Toxicology and Experimental Medicine, Hannover, Germany

A B S T R A C T

The interim results from this 90-day multi-dose, inhalation toxicology study with life-time post-exposure observation has shown an important fundamental difference in persistence and pathological response in the lung between brake dust derived from brake-pads manufactured with chrysotile, TiO_2 or chrysotile alone in comparison to the amphiboles, crocidolite and amosite asbestos.

In the brake dust exposure groups no significant pathological response was observed at any time. Slight macrophage accumulation of particles was noted. Wagner-scores, were from 1 to 2 (1 = air-control group) and were similar to the TiO_2 group.

Chrysotile being biodegradable, shows a weakening of its matrix and breaking into short fibers & particles that can be cleared by alveolar macrophages and continued dissolution. In the chrysotile exposure groups, particle laden macrophage accumulation was noted leading to a slight interstitial inflammatory response (Wagner-score 1–3). There was no peribronchiolar inflammation and occasional very slight interstitial fibrosis.

The histopathology and the confocal analyses clearly differentiate the pathological response from amphibole asbestos, crocidolite and amosite, compared to that from the brake dust and chrysotile. Both crocidolite and amosite induced persistent inflammation, microgranulomas, and fibrosis (Wagner-scores 4), which persisted through the post exposure period. The confocal microscopy of the lung and snap-frozen chestwalls quantified the extensive inflammatory response and collagen development in the lung and on the visceral and parietal surfaces.

The interim results reported here, provide a clear basis for differentiating the effects from brake dust exposure from those following amphibole asbestos exposure. The subsequent results through life-time post-exposure will follow.

1. Introduction

This study was designed to evaluate the hypothesis of whether brake dust from chrysotile containing brake drums will produce a pathological response following sub-chronic inhalation exposure in rats with a post-exposure observation period through the rat's lifetime.[1] Previous studies of brake dust containing chrysotile (Bernstein et al., 2014, 2015 & Bernstein et al., 2018) have shown that the brake dust produces no pathological response in the respiratory tract or pleura following inhalation either in a short term 5 day exposure (exposure concentration 46 WHO[2] f/cm^3) and or a 28 day exposure (exposure concentrations 7, 15, 24 WHO f/cm^3)(WHO, 1985). These studies have shown as well that the chrysotile used in the brake dust has minimal effect, while the amphibole asbestos, crocidolite, produced significant pathological response in both the lung and pleural cavity. The 90-day sub-chronic inhalation toxicity study is often a pivotal study for assessing no-effect

DOI of original article: https://doi.org/10.1016/j.taap.2019.114856
* Corresponding author at: 40 chemin de la Petite-Boissière, Geneva 1208, Switzerland.
E-mail address: davidb@itox.ch (D.M. Bernstein).
[1] The study was terminated when ~20% of the rats were remaining in one of the exposure groups.
[2] WHO fibers: Fibers with length > 5 μm, diameter < 3 μm and aspect ration of 3:1 (WHO, 1985)

https://doi.org/10.1016/j.taap.2019.114847
Received 23 August 2019; Received in revised form 28 November 2019; Accepted 1 December 2019
Available online 09 December 2019

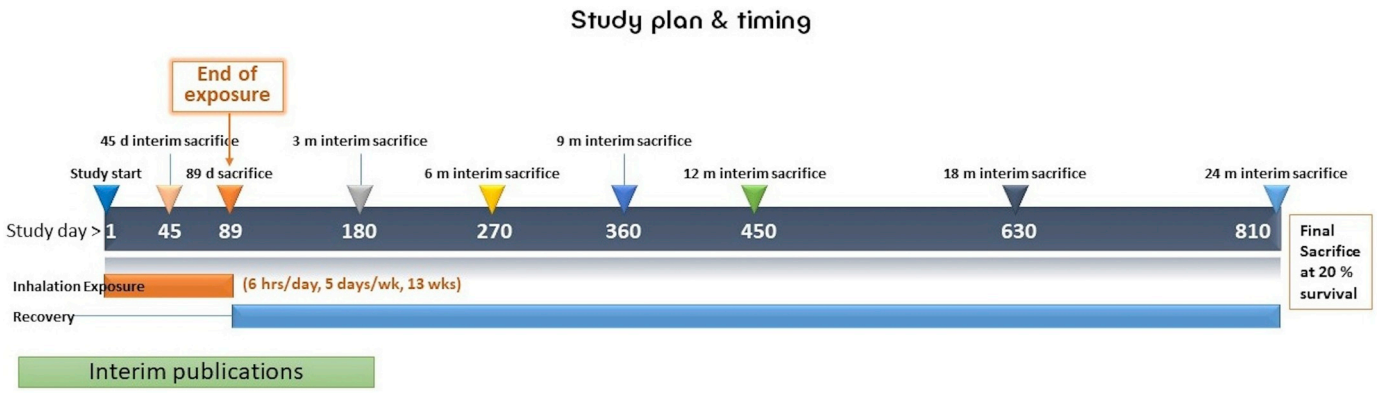

Fig. 1. Study plan and timing for the sub-chronic inhalation toxicology study.

levels as well as longer term toxicity. The standard protocol design for a 90-day sub-chronic inhalation toxicity study specifies a non-exposure recovery period of up to 4 weeks (OECD 413, 2018; EPA 712–C–98–204, 1998). As fiber related disease in humans has a long latency period, to fully assess the long-term potential of the fibers to cause disease, the study was designed with a life-time non-exposure period[1]. With 9 exposure groups and multiple endpoints, the results from this study are presented in two publications due to the extensive amount of data and results. Part 1 (Bernstein et al., 2019) provides the methods and results from the experimental design, aerosol exposure, lung burdens and the bronchoalveolar lavage results. Part 2 presented here presents the methods and results from the histopathological examination of the lungs and the confocal microscopy examination of the lung and the pleural cavity. In addition, the fibrosis quantification performed as part of the histopathology examination and the collagen quantification of the lung and pleura as performed by confocal examination are presented.

The confocal microscopy examination and analysis has been included in addition to the histopathological examination as it provides an in situ three-dimensional image of the tissue and possible pathology present in the lung and pleural cavity as well as the number and length of fibers in these regions. In addition, it provides a quantitative assessment of the amount of collagen present in the lung and in the visceral and parietal pleura (Rogers, 1999).

2. Methods

The experimental design, inhalation exposure, sampling, lung digestion fiber counting and sizing methodology and the bronchoalveolar lavage methods have been presented in Part 1 (Bernstein et al., 2019).

The experimental design study plan and timing of the exposure and non-exposure recovery period is shown in Fig. 1. The interim sacrifices are indicated on top of the time-line bar. The time-line bar shows the study day referred to herein. The timing of the inhalation and exposure period are shown below. The current interim publications cover the results through 180 days (3 months post-exposure) with the exception of the BAL results for which a few additional time points are included as this was readily processed and includes the full set of data on BAL.

The following summarizes the study protocol and endpoints.

Groups of laboratory rats were exposed by inhalation for 6 h per day 5 days per week for 13 weeks. Different subsets of animals were scheduled to be sacrificed immediately following 45 and 89 days of exposure (approximately 0.2–1 h after end of exposure) and at 3, 6, 9, 12, 18 and 24 months after the last exposure (experimental days 180, 270, 360, 450, 540). The final sacrifice is planned, when one of the groups reach 20% survival. The following groups were exposed (Table 1):

The following analyses were conducted for each group:

- Aerosol exposure characterization (presented in Part 1)
- Fiber / Particle lung burden evaluation (presented in Part 1)
- Bronchoalveolar lavage examination (presented in Part 1)
- Histopathology examination (presented in Part 2)
- Confocal microscopy of the lung including collagen quantification (presented in Part 2)
- Confocal low temperature microscopy of the lung and chestwall including collagen quantification (presented in Part 2)

2.1.1. *Tissue preparation for histopathology and confocal microscopy*

In animals assigned for lung histopathology and confocal microscopy (4 rats/group), the lungs and the lower half of the trachea were collected with the attached mediastinal tissue. In addition, the diaphragm was collected for confocal microscopy. Macroscopic abnormalities of the lungs were recorded, and the lung weight measured and recorded.

2.1.2. *Histopathology*

The left lung lobe of each animal assigned to lung histopathology was fixed in 10%-neutral buffered formalin solution by gentle instillation (via trachea following tying off right mainstem bronchus) under a hydrostatic pressure of 25 cm. In addition, the LALN (lung-associated lymph nodes) were fixed separately. The lung was then immersion-fixed for at least 2 days in formalin similar to the other organs.

The histopathological examination followed the approach as developed in the previous 28 day brake dust study performed at Fraunhofer ITEM using both H&E and Mason's Trichrome stains. The Wagner score[3] was determined (McConnell and Davis, 2002). In addition, a semi-qualitative evaluation of the collagen deposition was performed (McConnell et al., 1999).

For histopathological evaluation, all prepared slides were transferred to Fraunhofer ITEM with appropriate documentation and details of the gross macroscopic findings. Histopathological observations were recorded using the PROVANTIS system (version 8.4.3.1 or higher). Findings were scored using a grading scale of:

- none (0) – no lesion present
- minimal or very slight (1) – lesion covering ~ up to 5% of the slide
- slight (2) – lesion covering ~ up to 25% of the slide
- moderate (3) – lesion covering ~ up to 50% of the slide
- and severe (4) – lesion covering ~ 50–75% of the slide

These are approximate ranges and may vary depending upon the lesion type.

[3] Grade 1 = No lesion observed.

Table 1
Exposure groups, mean gravimetric and fiber concentrations (WHO fibers & Fibers L > 20 μm)[a].

	Mean gravimetric concentration	Mean fiber concentration	
Exposure group	mg/m^3	WHO fibers/cm^3	fibers L > 20μm/cm^3
Group 1: Air Control (Filtered air alone)	–	0.15	0
Group 2: Low dose (LD) level of brake dust	0.20	2.42	0.17
Group 3: Mid dose (MD) level of brake dust	0.34	4.85	0.43
Group 4: High dose (HD) level of brake dust	0.67	6.63	0.52
Group 5: Titanium dioxide (TiO_2) particle control	0.70	0.33	0
Group 6: Low dose level of Chrysotile 7H19	0.27	119	28.38
Group 7: High dose level of Chrysotile 7H19	0.64	233	72.33
Group 8: High dose level of Crocidolite asbestos (Voorspoed mine)	1.28	181	23.5
Group 9: High dose level of Amosite asbestos	2.32	281	47.66

[a] The WHO fibers & Fibers L > 20 μm are shown here, all fiber length categories are presented in Part 1 (Bernstein et al., 2019a).

2.1.3. Confocal microscopy

The right lung lobes of each animal assigned to lung histopathology/confocal microscopy were fixed in modified Karnovsky fixative made with Phosphate Buffered Saline by gentle instillation under a hydrostatic pressure of 25 cm. The diaphragm was also fixed in modified Karnovsky. The tissues were then immersion-fixed for at least 2 days.

Tissue preparation for lung burden measurements: In the animals assigned for lung burden analysis (4 rats/group), rats were sacrificed, the abdominal cavity was opened, and the diaphragm from the chest wall was excised (scalpel and forceps) at the insertion boundary of the chest wall along the entire circumference of contact between the chest wall and the diaphragm. The entire diaphragm was removed intact avoiding touching the parietal surface and placed in a new clean bottle/vial, capped, sealed, labelled and then quickly deep frozen at -80 °C. The upper half of the trachea, the lungs, and the lower half of the trachea were also collected with the attached mediastinal tissue. The mediastinal lymph nodes and the tracheobronchial lymph nodes were resected and immediately inserted into appropriate labelled plastic bags and quickly deep-frozen at -80 °C.

The deep-frozen tissue samples were dispatched for freeze drying and low temperature ashing on dry ice to the Inhalation Toxicology & Chemical Risk Assessment department of the Fraunhofer Institute, Hannover, Germany. Following this, Fraunhofer sent the ashed diaphragms to GSA for fiber counting and sizing.

Tissue preparation for confocal / low temperature microscopy: On days 45 and 89 during exposure and at 3, 9, 12 and 18 months post-exposure, for 4 animals per group, chestwalls were prepared without delay upon animal termination by overdose of sodium pentobarbital and exsanguination via peritoneal incision of the liver with care taken not to invade the lung cavity or puncture the diaphragm. A short length of PE 190 tubing was inserted into the trachea proximal to the brachial plexus and secured with silk suture. The chest wall was skinned and separated and was suspended at the neck region and slowly lowered over 1 min into liquid nitrogen with care taken not to submerge the open end of the tracheal tube into the liquid nitrogen. The snap-frozen chest walls were then bagged and numbered for low temporary storage at −80 °C. The frozen chest walls were then dispatched packed on dry ice by express courier to Rogers Imaging Corporation (RIC) for processing and analysis. Upon receipt, chestwalls were inventoried and maintained on dry ice. Individual chestwalls were positioned on a dry ice-cooled copper plate cutting platform mounted on a thin-kerf band saw. Beginning at the xyphoid process, sequential cross section chestwall slabs 4 mm thick were cut using a band saw toward the brachial plexus until no lung profile remained. Every cut slab was immediately place on dry ice until positioned in a tissue processing cassette. Cassettes were placed in cryofixation solution containing anhydrous Methanol and anhydrous Acetone in a mixture of three parts Methanol to one part Acetone at −80 °C, then placed in an ultralow freezer maintained at −80 °C. Cryofixation fluid was replaced periodically until no free ice crystals remained. Cassettes were then placed in cryofluid containers maintained at −20 °C. Cryofluid was weekly replaced until solution cleared, then cassettes were transferred to anhydrous methanol for two weeks with several changes in methanol, transferred to −4 °C, then brought to room temperature in absolute methanol on stir plate. Methanol was replaced with anhydrous methanol containing 0.0001% Lucifer yellow-CH (Electron Microscopy Sciences, Erie, PA) for 48 h. Stained chestwall slabs were placed in fresh methanol and embedded in Spurr epoxy. Embedded chestwall slabs were prepared for microscopic analysis by removal of the top 1.5 mm from the block, then the chestwall surface was polished to a glass smooth finish using a diamond lapidary tool. Polished chestwall slabs were then cover-slipped and placed on the microscope stage for examination. The chestwall processing and confocal image collection and analysis is described in Bernstein et al. (2018).

2.2. Statistical analyses

One-way ANOVA followed by Dunnett's multiple comparisons test was performed using GraphPad Prism version 8.1.2 for Windows, GraphPad Software, San Diego, California USA, www.graphpad.com".

Graphs and summary statistics were prepared using STATISTICA (data analysis software system), TIBCO Software Inc. (2018) http://tibco.com.

3. Results

3.1. Lung weights

At necropsy, the lung weight of each animal was measured and recorded as well as the terminal body weight. The mean and standard deviation of the lung weight/ body weight ratio are shown in Table 2. Statistically significant increases were seen in Groups 8 and 9 at 45, 89 and 180 days, which indicated that the lungs were approximately 20% heavier than the control group most likely as a result of the inflammatory response to these fibers. The ANOVA analysis and the full statistical comparisons are presented in Section S-1 (supplemental data).

3.2. Histopathology

The histopathological findings in the lung are presented in the Section S-2 (supplemental data) with key histopathological scores illustrated in Fig. 2.[4] Representative histopathological images are

[4] Histopathology scoring using a grading scale of none (0), minimal (1), slight (2), mild (3), and severe (4). The numbers shown in Figure 1 are the histopathology score X the number of animals with that score (e.g. 2 rats with slight (2) findings = 4).

Table 2
Percent lung weight/body weight (ratio) at necropsy (Means / Standard deviations).

Group	1	2	3	4	5	6	7	8	9
45 days									
Mean	0.3875	0.3625	0.3675	0.3538	0.3538	0.4038	0.4125	0.4625*	0.4663*
Std. Deviation (No)	0.03536 (8)	0.05175 (8)	0.03151 (8)	0.01768 (8)	0.03739 (8)	0.03292 (8)	0.03536 (8)	0.07440 (8)	0.04838 (8)
89 days									
Mean	0.3860	0.3460	0.3600	0.3760	0.3480	0.3780	0.3680	0.4480*	0.4620*
Std. Deviation (No)	0.03435 (5)	0.03209 (5)	0.04183 (5)	0.02608 (5)	0.01789 (5)	0.02168 (5)	0.03033 (5)	0.03962 (5)	0.03564 (5)
180 days									
Mean	0.3000	0.2800	0.2800	0.2850	0.2938	0.3300	0.3038	0.3588*	0.3988*
Std. Deviation (No)	0.03117 (8)	0.03780 (8)	0.04957 (8)	0.04071 (8)	0.02504 (8)	0.03464 (8)	0.01685 (8)	0.05139 (8)	0.02295 (8)

(Groups: 1- Air control; 2-Low dose BD; 3-mid dose BD; 4-high dose BD; 5-TiO2; 6-low dose chrysotile; 7-high dose chrysotile; 8-crocidolite; 9-amosite).
* Statistically significant as compared to the controls (Dunnet's test/ANOVA).

presented in Section S-3 (supplemental data). These findings clearly differentiated the response to brake dust as compared to chrysotile, crocidolite and amosite asbestos.

There were no exposure-related histopathological findings in animals exposed to filtered air at any time point.

(Multi)focal very slight (minimal) alveolar/interstitial accumulation of particle-laden macrophages (alveolar histiocytosis), predominantly at bronchiolo-alveolar junctions was observed in response to the particles in the brake dust groups at 45, 89 and 180 days. This finding was also observed in the TiO_2 particle control group. At 180 days, the incidences of (multi)focal very slight to slight accumulation of particle- or fiber-laden macrophages in the BALT (bronchus-associated lymphoid tissue) were increased as compared to the previous sacrifices in both the brake dust and TiO_2 groups. The BALT is the lymphatic sump below the bronchial bifurcations, which accumulate particles cleared by the lymphatic system.

In the chrysotile exposed groups, (multi)focal very slight (minimal) alveolar/interstitial accumulation of particle-laden macrophages (alveolar histiocytosis), predominantly at bronchiolo-alveolar junctions were also observed at 45, 89 and 180 days due to the large number of

# animals x score	0	1	2	3	4	5	6	7	8

Exposure group	Control	Control	Control	Brake dust low	Brake dust low	Brake dust low	Brake dust mid	Brake dust mid	Brake dust mid	Brake dust high	Brake dust high	Brake dust high	TiO_2	TiO_2	TiO_2
Time	45 d	89 d	180 d	45 d	89 d	180 d	45 d	89 d	180 d	45 d	89 d	180 d	45 d	89 d	180 d
Histopathological findings															
Accumulation, Particle-Laden Macrophages, Alveolar/Interstitial	0	0	0	4	4	4	4	4	4	4	4	4	5	5	4
Accumulation, Fibre-Laden Macrophages, Alveolar/Interstitial	0	0	0	0	0	0	0	0	0	0	0	0	0	0	0
Fibrosis, Interstitial	0	0	0	0	0	1	0	0	0	0	0	0	0	0	0
Fibrosis, Pleural	0	0	0	0	0	1	0	0	0	0	0	0	0	0	1
Giant Cells, Syncytial	0	0	0	0	0	0	0	0	0	0	0	0	0	0	0
Hyperplasia, Bronchiolo-Alveolar	1	0	1	0	0	0	0	1	2	0	1	0	0	0	1
Infiltration, Inflammatory Cell, Peribronchiolar	0	0	0	0	0	0	0	0	0	0	0	0	0	0	0
Infiltration, Inflammatory Cell, Perivascular	0	0	0	1	2	3	1	2	0	1	0	2	0	2	0
Infiltration, Inflammatory Cell, Pleural	0	0	0	0	0	0	0	0	1	0	0	0	0	0	0
Infiltration, Inflammatory Cell, Alveolar/Interstitial	0	0	0	0	0	0	0	0	0	0	0	0	0	1	0
Macrophage Aggregation, Alveolar	0	0	1	0	0	0	0	0	0	0	0	0	0	0	0
Microgranuloma	0	0	0	0	0	0	0	0	0	0	0	0	0	0	0
Accumulation, Particle-Laden Macrophages, Balt	0	0	0	0	0	2	0	0	3	0	0	2	1	0	4
Accumulation, Fibre-Laden Macrophages, Balt	0	0	0	0	0	0	0	0	0	0	0	0	0	0	0
Lung associated lymph nodes (LALN)															
Accumulation, Particle-Laden Macrophages	0	0	0	1	0	3	1	1	3	1	1	3	1	1	2
Accumulation, Fibre-Laden Macrophages	0	0	0	0	0	0	0	0	0	0	0	0	0	0	0

Exposure group	Chrysotile low	Chrysotile low	Chrysotile low	Chrysotile high	Chrysotile high	Chrysotile high	Crocidolite	Crocidolite	Crocidolite	Amosite	Amosite	Amosite
Time	45 d	89 d	180 d	45 d	89 d	180 d	45 d	89 d	180 d	45 d	89 d	180 d
Histopathological findings												
Accumulation, Particle-Laden Macrophages, Alveolar/Interstitial	4	4	4	4	4	4	0	0	0	0	0	0
Accumulation, Fiber-Laden Macrophages, Alveolar/Interstitial	0	0	0	0	0	0	6	8	8	8	8	8
Fibrosis, Interstitial	0	0	0	0	2	4	4	5	8	4	8	8
Fibrosis, Pleural	2	0	0	0	0	1	1	0	1	1	1	2
Giant Cells, Syncytial	0	0	0	1	1	0	3	4	5	4	6	8
Hyperplasia, Bronchiolo-Alveolar	2	4	4	4	4	4	8	8	8	8	8	8
Infiltration, Inflammatory Cell, Peribronchiolar	0	0	0	0	1	1	8	5	5	7	5	6
Infiltration, Inflammatory Cell, Perivascular	1	3	4	2	3	2	5	4	5	5	4	6
Infiltration, Inflammatory Cell, Pleural	0	0	0	0	0	1	0	0	0	1	0	0
Infiltration, Inflammatory Cell, Alveolar/Interstitial	0	3	2	0	4	4	5	8	8	8	8	8
Macrophage Aggregation, Alveolar	0	0	0	0	0	0	0	0	0	0	0	0
Microgranuloma	2	4	3	4	2	4	8	8	8	8	8	8
Accumulation, Particle-Laden Macrophages, Balt	1	0	4	0	0	4	0	0	0	0	0	0
Accumulation, Fibre-Laden Macrophages, Balt	0	0	0	0	0	0	0	1	4	0	1	4
Lung associated lymph nodes (LALN)												
Accumulation, Particle-Laden Macrophages	1	2	4	0	0	3	0	0	0	0	0	0
Accumulation, Fibre-Laden Macrophages	0	0	0	0	0	0	0	3	6	1	2	4

Fig. 2. Summary of histopathological findings at 45, 89 (end of exposure) and 180 days. The individual results are presented in Section S-2 (supplementary data). The score shown is the product of the number of animals with the finding (from 0 to 4) and the grade for each animal (from 0 to 2) and ranged from 0 to 8. The grading system used for evaluation ranged as follows: 1) very slight/minimal, 2) slight, 3) moderate, 4) severe, 5) very severe. Eg: Group with 2 rats of score of 1 would be shown as 2. The colour scheme used in the table is as follows:

particles and shorter fibers present in the aerosol. Multifocal very slight microgranulomas at bronchiolo-alveolar junctions were diagnosed in rats each of group 6 (Chrysotile low) and 7 (Chrysotile high) at 89 and 180 days. At 89 and 180 days, multifocal interstitial fibrosis was seen in 2/4 rats of group 7 (Chrysotile high; all very slight).

In the crocidolite and amosite exposure groups at 45 days (multi) focal very slight (minimal) alveolar /interstitial accumulation of fiber-laden macrophages (alveolar histiocytosis), were seen predominantly at the bronchiolo-alveolar junctions. In addition, this was accompanied by (multi)focal peribronchial /peribronchiolar and alveolar/interstitial (intraseptal) infiltration of (mixed) inflammatory cells with multifocal slight microgranulomas at bronchiolo-alveolar junctions. Multifocal very slight interstitial fibrosis was observed in all rats.

These findings persisted though 89 days. In addition, (multi)focal occurrence of multinucleated (syncytial) giant cells and (multi)focal peribronchial/peribronchiolar infiltration of (mixed) inflammatory cells was observed in all rats at 89 days. The multifocal interstitial fibrosis also persisted in all rats.

By 180 days (90 days post exposure), (multi)focal interstitial fibrosis (slight) was seen in all rats of the crocidolite and amosite exposure groups.

The Wagner scores are shown in Fig. 3. The Wagner grading system made a clear differentiation (brake) between Grade 3 and Grades 4–8, with the former representing “cellular change” (inflammatory and reversible) and the latter progressive degrees of fibrosis (not totally reversible) (McConnell and Davis, 2002). In all brake-dust groups, grades 1 and 2 were observed reflecting the normal macrophage clearance of the particles. In the chrysotile low dose exposed group, grades 2 and 3 were observed at 45 days and grade 3 at 89 and 180 days reflecting the increased cellular activity in response to the higher fiber exposure. In the chrysotile high dose exposure group, grade 3 was observed at 45 and 180 days, while at 89 days (end of exposure) 2 rats were grade 3 and 2 rats were grade 4. The quantification analysis performed by Fraunhofer indicated that at 89 days fibrosis was observed in a mean of 0.28% of the histopathological slide examined (Table 3).

In the crocidolite and amosite exposed groups grade 4 was observed at all time points (45, 89 & 180 days, Fig. 2). This reflected the persistence of the insoluble crocidolite fibers in the lung, which appear to continue to stimulate the inflammatory response of the lung resulting in increased fibrosis. The quantification analysis performed by Fraunhofer as shown in Table 3, indicated that collagen progressively increased in the crocidolite group from a mean of 0.43% at 45 days to 1.05% at 180 days and in the amosite group from 0.77% at 45 days to 1.10% at 180 days.

At histopathological examination, the only observed epithelial change in the lungs was (multi)focal bronchiolo-alveolar (b.-a.) hyperplasia of the bronchiolar type (synonym: alveolar bronchiolization). This type of hyperplasia describes the presence of bronchiolar epithelium within alveolar ducts and adjacent alveoli. It is commonly seen in particle- and fiber-inhalation studies and interpreted as an attempt to increase particle−/fiber-removalfrom the lungs by extension of the so-called “mucociliary escalator“. Alveolar bronchiolization is not considered a pre-neoplastic lesion, even if graded severe. In contrast, in the present study, this change was graded no more than very slight or slight in any group or at any examination timepoint. Other types of epithelial hyperplasia such as alveolar type II cell hyperplasia (b.-a. hyperplasia of the alveolar type) or b.-a. hyperplasia of the mixed type (mixture of bronchiolar and alveolar type II cells), which at a severe degree of severity are of more concern regarding a potential pre-neoplastic character, were not observed at all throughout the study. The same refers to epithelial cell metaplasia, e.g. squamous cell metaplasia.

Histologically, there was also no occurrence of mesothelial cell hyperplasia (proliferation of pleural mesothelial cells) in the present study. However, this does not exclude the occurrence of focal mesothelial hypertrophy (activated mesothelial cells), which may be recognizable at the electron microscopic level.

Table 3
Fibrosis quantification analysis performed by Fraunhoferon histopathology slides (percentage of the number of grids on the slide with fibrosis)*.

Group	45 days	89 days (end of exposure)	180 days
Brake dust low, med, high	0	0	0
TiO_2	0	0	0
Chrysotile low dose	0	0	0
Chrysotile high dose	0	0.28	0
Crocidolite	0.43	0.75	1.05
Amosite	0.77	0.99	1.10

* The findings reflect the presence and intensity of fibrotic response.

3.3. Confocal microscopy: pathological response in the lung

The spatial and temporal distribution of test article and the associated inflammatory responses in lungs of the rats was assessed using multiplexed confocal microscope analyses. In addition, the amount of collagen in the connective tissue in the lung parenchyma was determined in each group at 45, 89 and 180 days. The mean percent collagen in the lung as determined by confocal microscopy at the 45 days, 89 days (end of exposure) and at 180 days (90 days post exposure) are shown in Fig. 4.

No statistically significant differences were observed in the percent collagen in the lungs for the brake-dust groups, the TiO_2 group or the chrysotile groups as compared to the controls.

At 45, 89 and 180 days, the mean percent collagen in the lung in both the crocidolite and amosite groups was increased (statistically

Exposure group / Time / Wagner score	Control 45 d	Control 90 d	Control 3 m	Brake dust low 45 d	Brake dust low 90 d	Brake dust low 3 m	Brake dust mid 45 d	Brake dust mid 90 d	Brake dust mid 3 m	Brake dust high 45 d	Brake dust high 90 d	Brake dust high 3 m	TiO2 45 d	TiO2 90 d	TiO2 3 m
Wagner Grade 1	4	4	4	0	0	0	0	0	0	0	0	0	0	0	0
Wagner Grade 2	0	0	0	4	4	4	4	4	4	4	4	4	4	4	4
Wagner Grade 3	0	0	0	0	0	0	0	0	0	0	0	0	0	0	0
Wagner Grade 4	0	0	0	0	0	0	0	0	0	0	0	0	0	0	0

Exposure group / Time / Wagner score	Chrysotile low 45 d	Chrysotile low 90 d	Chrysotile low 3 m	Chrysotile high 45 d	Chrysotile high 90 d	Chrysotile high 3 m	Crocidolite 45 d	Crocidolite 90 d	Crocidolite 3 m	Amosite 45 d	Amosite 90 d	Amosite 3 m
Wagner Grade 1	0	0	0	0	0	0	0	0	0	0	0	0
Wagner Grade 2	2	0	0	0	0	0	0	0	0	0	0	0
Wagner Grade 3	2	4	4	4	2	4	0	0	0	0	0	0
Wagner Grade 4	0	0	0	0	2	0	4	4	4	4	4	4

Fig. 3. Wagner scores for each group. The number shown is the number of animals for each group/time point with that Wagner score.

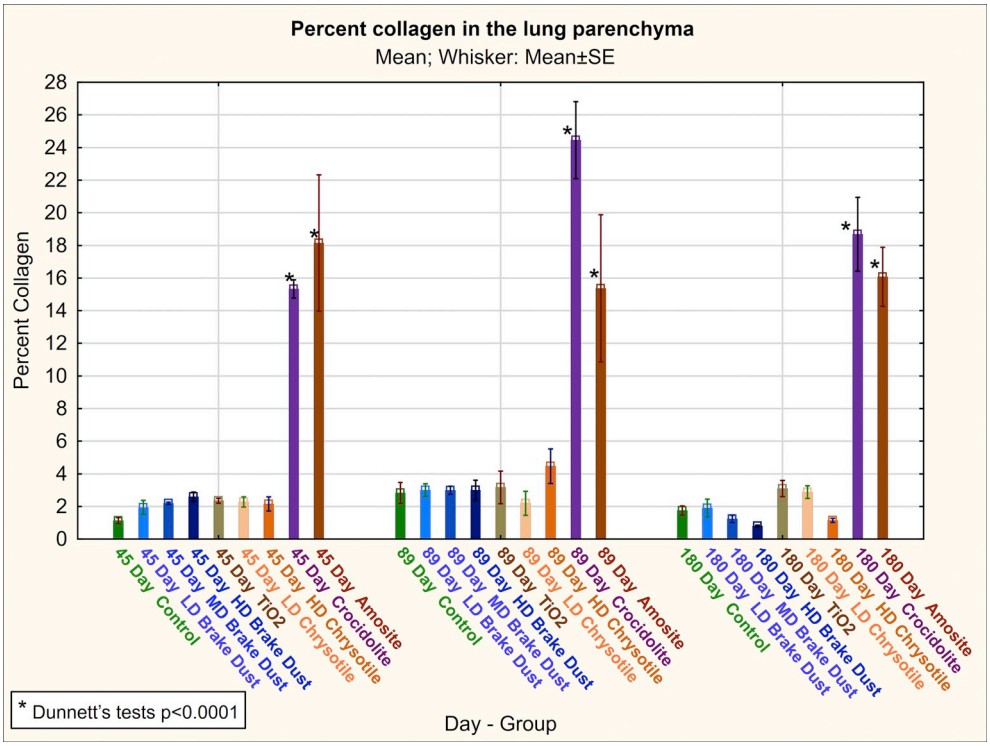

Fig. 4. Confocal microscopy – Lung Parenchyma Percent Collagen (Percent collagen = volume of the parenchyma collagen/volume of parenchyma tissue × 100) shown by group and day (Means ± SE).

significant, $p < .0001$) as compare to the controls at each time point. For crocidolite the increase ranged from 14 to 21% and for amosite from 11 to 14%. The one-way ANOVA analysis and the results of the Dunnett's tests are presented in Section S-4 (supplementary data).

With the confocal analysis of the lung, the length of any fibers observed within the volume of tissue analyzed was also recorded. Based upon the number of fibers observed in these volumes, an estimate was made of the total possible number of fibers per cm^3 of the lung tissue (Fig. 5). This estimate was based upon the number of fibers per tissue volume determined and then extrapolated to the total lung volume. The

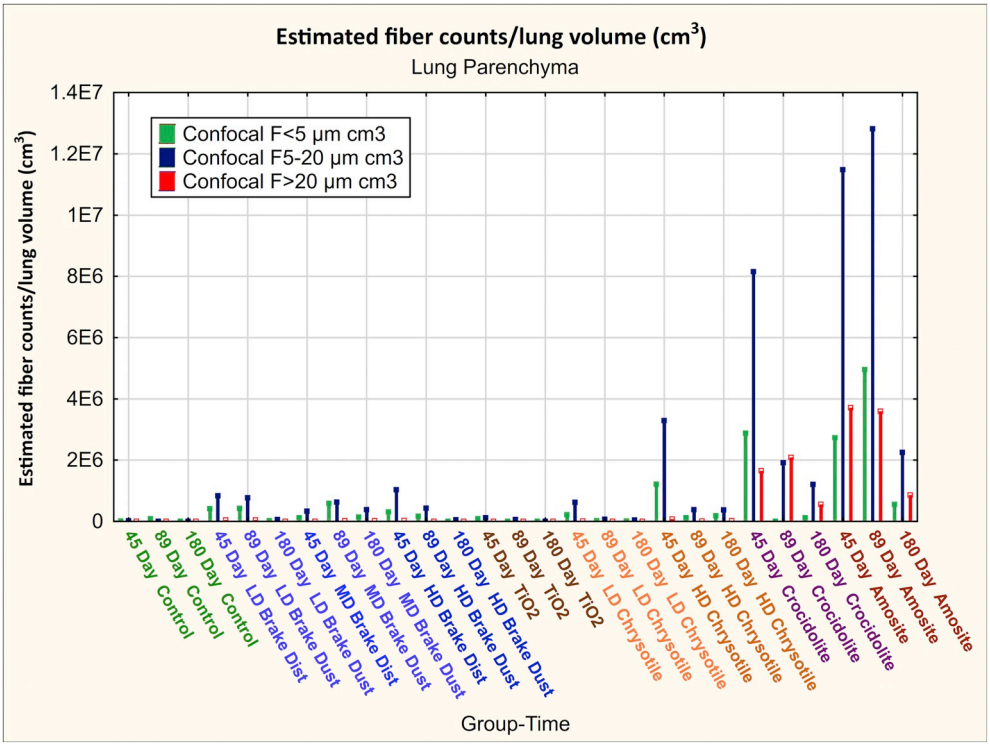

Fig. 5. Confocal microscopy – Estimated fiber counts/lung volume (cm^3). The estimated fiber counts are shown for the size ranges < 5 µm, 5–20 µm and > 20 µm for each group and time point.

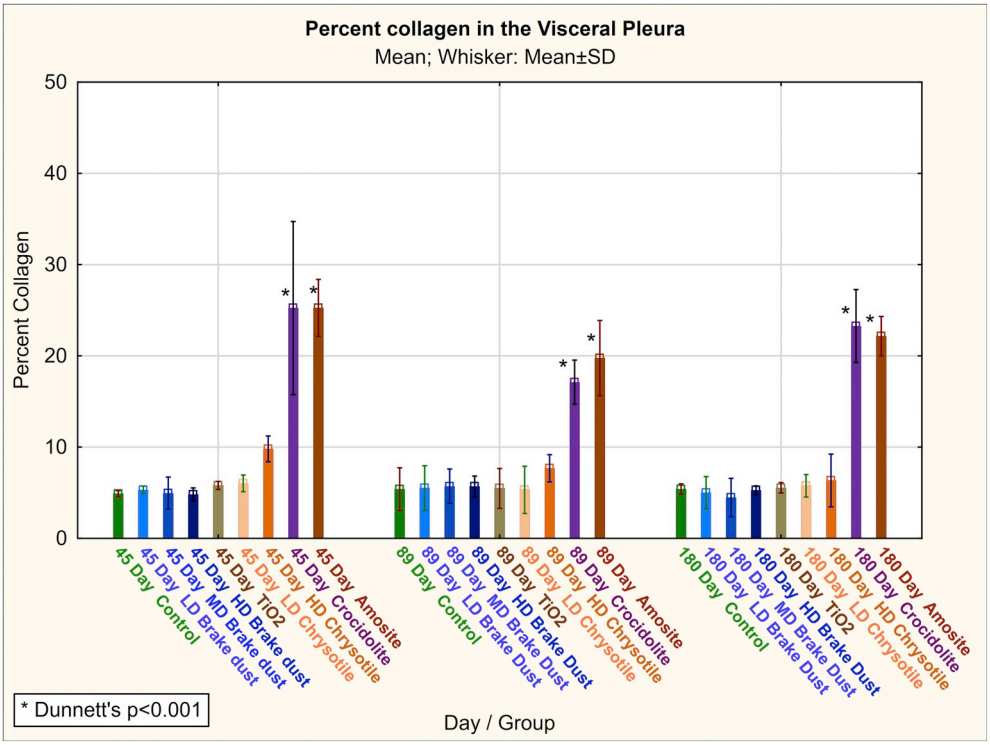

Fig. 6. Confocal microscopy quantification of the percent collagen in the visceral pleura (Percent collagen = volume of collagen/volume of visceral pleural tissue × 100) shown by group and day (Means ± SD).

airways and parenchyma were assessed separately. In the large conducting airways, few if any fibers were found suggesting that the large majority were rat respirable. In the lung parenchyma, the fibrous shaped objects observed in the air control and TiO_2 were not chrysotile. In the brake dust groups and in the chrysotile exposed animals, the majority of fibers observed in the lung parenchyma were in the range of < 5 μm and 5–20 μm lengths with few fibers > 20 μm found. In the crocidolite and amosite exposed animals, more fibers were observed in each category and especially fibers longer than 20 μm.

3.4. Confocal microscopy - Pathological response in the pleural cavity

The mean percent collagen / connective tissue in the visceral and parietal pleural as determined by confocal microscopy at 45 days, at the end of exposure (experimental day 89) and at 3 months post exposure (experimental day 180) are shown in Figs. 6 and 7. No statistically significant differences were observed in either the visceral or parietal pleural percent collagen / connective tissue for the brake-dust, TiO_2 or chrysotile exposed animals as compared to the controls. At all three time points (45, 89 and 180 days), both the visceral and parietal pleural percent collagen / connective tissue of the crocidolite and the amosite exposed animals were significantly increased as compared to the control group ($p < .0001$, ANOVA/Dunnett's test). For crocidolite the mean increase over 45, 89 and 180 days compared to the control group was 2.8 times in the visceral pleura and 3.4 times in the parietal pleura. For amosite the mean increase over 45, 89 and 180 days compared to the control group was 3.9 times in the visceral pleura and 3.0 times in the parietal pleura. The statistical comparison between groups and time points is presented in Section S-5 (supplemental data).

3.5. Confocal microscopy images of the lung

The lungs that were collected from animals in each group at 45 days, the end of exposure at 89 days (experimental day 89) and at 3 months post exposure (experimental day 180) were processed as described in the methods and imaged using confocal microscopy. This process preserved the tissue, cellular and spatial orientation of any particles or fibers present in the lung.

Maximum intensity projections made from three dimensionally reconstructed serial section stacks of image data and 3D projection images selected from randomly recorded fields-of-view obtained from parenchyma and airway regions of lung from Groups 1 through 9 at each time point.

3.6. At 45 days

The normal parenchyma, alveolar region from Group 1, air control at 45 days is shown in Fig. 8, Panel 1. The bright green structures are connective tissue cables surrounding the alveoli. A few macrophages are present as well as a blood vessel. Group 2, brake dust low dose (Fig. 8, Panel 2) shows a normal conducting airway with alveoli on the exterior side. A few chrysotile fibers are present, one with a macrophage and another that was recorded as > 20 μm (the original Confocal images showed that the fiber was at an angle to the plane of the image and thus appears shorter).

Group 3 is not shown as it is similar to group 2 and 4. In Group 4, high dose brake dust (Fig. 8, Panel 3) a macrophage with particles is seen as well as a free-standing chrysotile fiber.

The TiO_2 particle control, Group 5 (Fig. 8, Panel 4) shows normal parenchyma, alveolar duct region, alveolar entrance. TiO_2 particles and macrophages are present including a macrophage, which has phagocytized numerous TiO_2 particles.

The chrysotile high dose, Group 7 (Fig. 8, Panel 5) shows normal parenchyma, alveolar duct region, alveolar entrance. Also present is a blood vessel and surrounding lymphatics. Numerous short chrysotile fibers and particles are seen with and without macrophages. The presence of such an accumulation of shorter fibers was unusual and may be a result of the longer chrysotile fibers breaking apart.

The amphibole asbestos groups 8 and 9 show a markedly different response. Fig. 8, Panel 6 (Group 8 crocidolite at 45 days) shows the lung

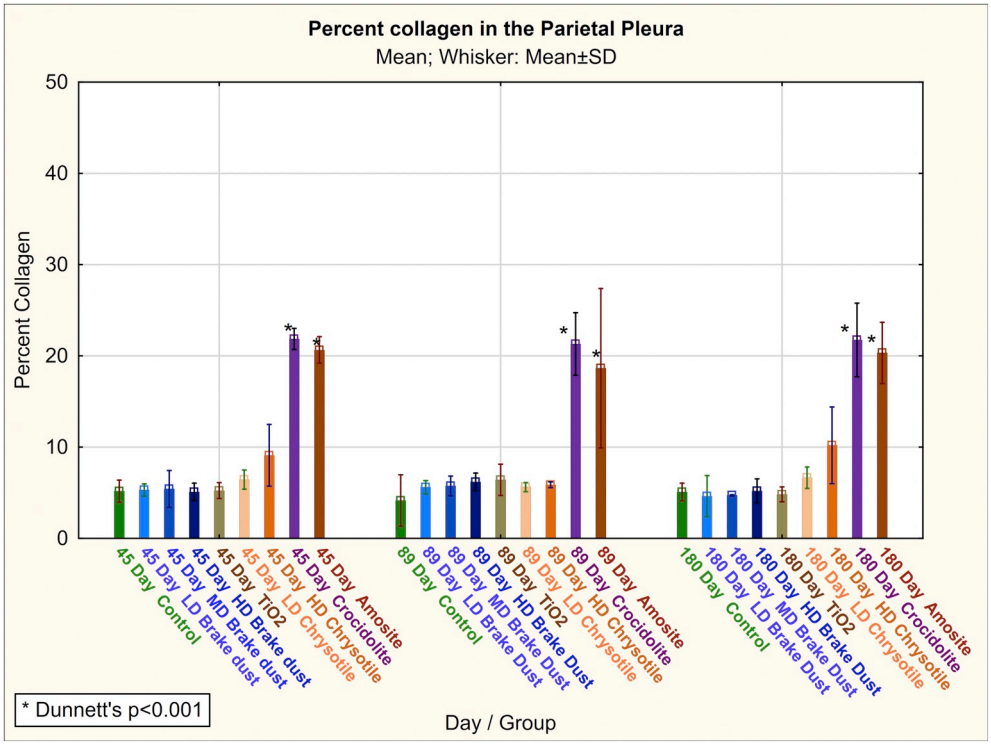

Fig. 7. Confocal microscopy qunatification of the percent collagen in the parietal pleura (Percent collagen = volume of collagen / volume of parietal pleural tissue x 100) shown by group and day (Means ± SD).

parenchyma, alveolar duct region, alveolar entrance. Large numbers of long (> 20 μm) and shorter crocidolite fibers are bound with alveolar macrophages forming granulomas. The developing collagen matrix in response to the fibers is also present. On the upper right of the image is a crocidolite fiber > 50 μm.

The amosite exposed lungs (Group 9 at 45 days) show a similar response as seen in Fig. 8, Panels 7 & 8. Numerous long and shorter amosite fibers, some longer than 40 μm, are present with alveolar macrophages and granulomas. An extensive collagen matrix has developed.

3.7. At 89 days

At the end of exposure (89 days), both the air control group 1 and the brake dust groups 2–4 were similar in appearance to that, which was observed at 45 days. A representative image of the brake dust groups at 89 days is shown in Fig. 9, Panel 1 for Group 3. Shown is an alveolar entrance in the normal parenchyma. A few short chrysotile fibers are observed, some with macrophages others free in the alveolus.

In the TiO_2 particle control group 89 days, Group 5 (Fig. 9, Panel 4) macrophages are observed with numerous TiO_2 particles.

The chrysotile high dose Group 7 at 89 days (Fig. 9, Panel 3) shows an alveolus with the cellular surface with chrysotile particles and short fibers present.

The particle effects seen in Groups 2–7 are contrasted with the long fiber (> 20 μm) effects seen in the amphibole Groups 8 and 9 at 89 days.

Fig. 9 Panel 4, shows a crocidolite exposed lung. On the right of the image is a conducting airway with an adjacent matrix of longer and shorter crocidolite fibers with localized connective tissue response within the interstitial spaces. The long fiber (> 20 μm) in the center is approximately 40 μm in length. On the left of the image is an alveolus with long crocidolite fibers (~30 μm) encapsulated in a granuloma.

An amosite exposed lung is shown in Fig. 9, Panel 5. In the lung parenchyma, numerous longer and shorter amosite fibers are associated with a localized connective tissue response. Present in the alveoli are long (~30 μm) amosite fibers encapsulated in giant cells / micro-granuloma. On the upper right of image is a blood vessel surrounded by distal lymphatics with amosite particles and short fibers.

3.8. At 180 days

At three months post exposure (180 days) the brake dust exposed groups (2–4) show occasional short fibers and/or macrophages in normal alveoli. A representative image from Group 4, high dose brake dust, is shown in Fig. 10, Panel 1, shorter fibers are sometimes seen free in the alveoli with an apparent protein coating (as indicated by the yellowish colour around the fiber).

At 180 days, the TiO_2 particle control Group 5 continues to show a macrophage response with macrophages occasionally present with numerous TiO_2 particles (Fig. 10, Panel 2).

In the chrysotile exposed Groups (6–7) at 180 days, macrophages and occasional clusters of macrophages are present in the alveoli some with short chrysotile fibers (Group 7: Fig. 10, Panel 3).

While the response to the exposure diminishes in groups 2–7 at three months post exposure, the amphibole Groups 8 & 9 show the opposite response with a continuing development of the collagen matrix in response to the longer and shorter fibers present.

Fig. 10, Panel 4 illustrates the extensive collagen adjacent to conducting airway, which developed following crocidolite exposure. Embedded in the interstitial connective tissue are numerous long and shorter crocidolite fibers.

Fig. 10, Panels 5 & 6 show the response to amosite asbestos at 180 days. In Panel 5, amosite fibers are seen penetrating and traversing the airway wall (center) with the interstitial connective tissue showing a localized collagen response. On the right is a granuloma with numbers amosite fibers present. In Panel 6, many long amosite fibers are present and are associated with either granuloma or an intensified collagen response.

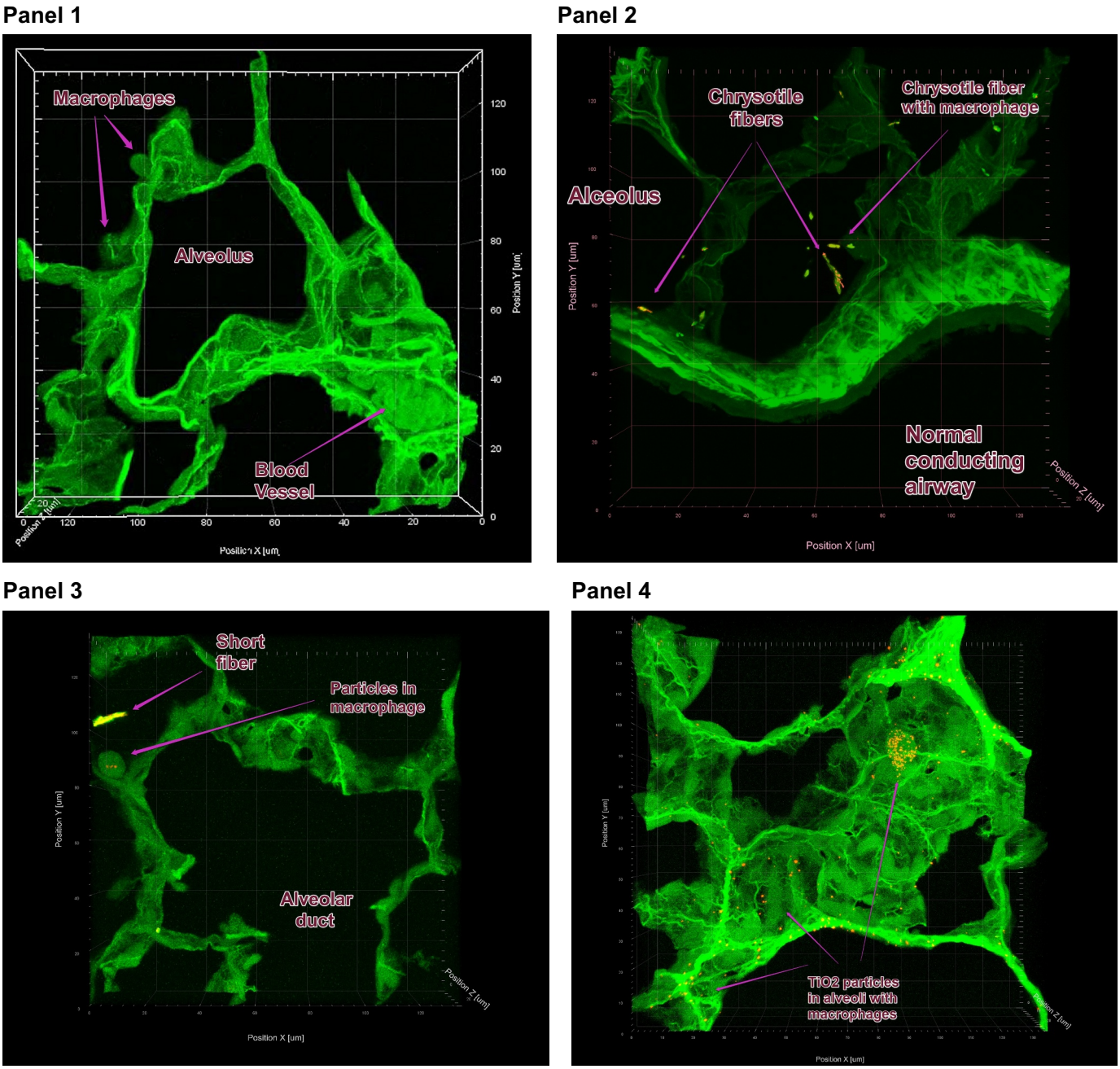

Fig. 8. Confocal images of the lung at 45 days: Bright green structures are connective tissue cables highlighted using maximum intensity projection from original image data. Particles and fibers are shown in orange. When protein coated, they appear yellow. These images are from projected three-dimensional reconstructions. The scale bars are in μm and are shown in each image in the surrounding frames.
Panel 1: Group 1, air control at 45 days: Shown are alveoli in normal parenchyma with macrophages.
Panel 2: Group 2, brake dust low dose at 45 days: Shown are alveoli in normal parenchyma with protein coated chrysotile fibers and a macrophage.
Panel 3: Group 4 Brake dust high dose at 45 days: Seen is normal parenchyma, showing an alveolar duct. A short fiber and a macrophage with particles are present.
Panel 4: Group 5, TiO_2 at 45 days: Normal Parenchyma, alveolar duct region, alveolar entrance. Shown are TiO_2 particles and a macrophage, which has phagocytized numerous TiO_2 particles.
Panel 5: Group 7, chrysotile high dose at 45 days. Shown is normal parenchyma, alveolar duct region, alveolar entrance. Also present is a blood vessel and surrounding lymphatics. Numerous short chrysotile fibers and particles are seen with a few macrophages.
Panel 6: Group 8, crocidolite at 45 days. Shown is the lung parenchyma, alveolar duct region, alveolar entrance. Large numbers of long and shorter crocidolite fibers are bound with alveolar macrophages forming granulomas. The developing collagen matrix is also present.
Panel 7: Group 9 amoiste at 45 days: Shown is a distal airway region of the lung parenchyma. Numerous long and shorter amosite fibers, some longer than 40 μm, are present with alveolar macrophages and granulomas. An extensive collagen matrix has developed.
Panel 8: Group 9, amosite at 45 days: Shown is the lung parenchyma, alveolar duct region, alveolar entrance. Numerous long and shorter amosite fibers are present with alveolar macrophages and granulomas. An extensive collagen matrix has developed. (For interpretation of the references to colour in this figure legend, the reader is referred to the web version of this article.)

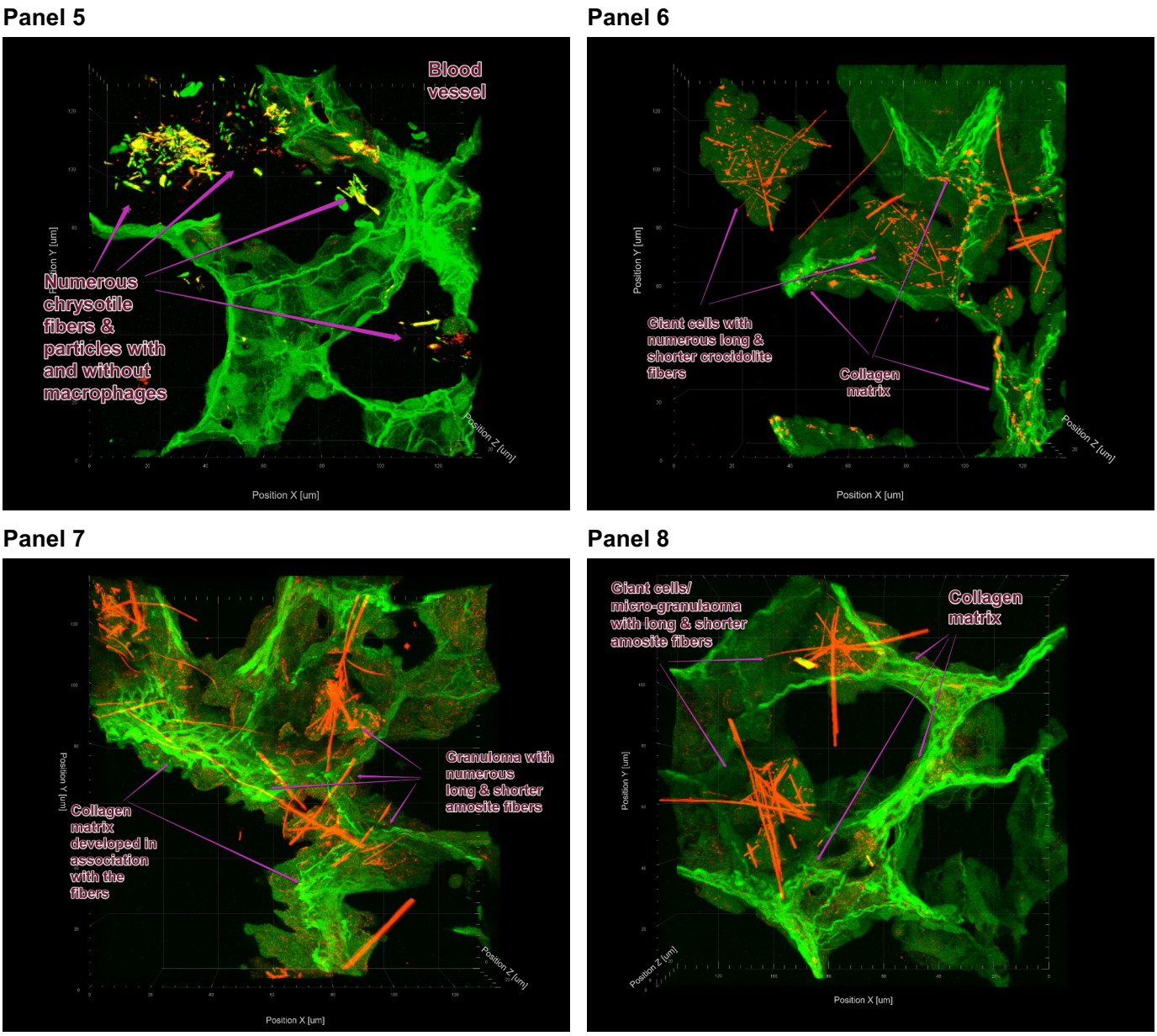

Fig. 8. (*continued*)

3.9. Confocal microscopy images of the pleura

The snap frozen chest walls that were collected from animals in each of groups at 45 days, the end of exposure (day 89) and at 3 months post exposure (day 180) were processed as described in the methods and imaged using confocal microscopy. This process preserved the tissue, cellular and spatial orientation of any particles or fibers present in the visceral and parietal pleura as well as in the pleural space. There was some minor contraction of the lung during the snap freezing process, which resulted in the wavy orientation of the visceral pleural surface.

The confocal microscopy images (Fig. 11) compare responses in the visceral and parietal pleura for each group. Sub-pleural alveolar septa appear as shades of green. Visceral pleural surface and (when present) parietal pleura surfaces high in collagen content appear as bright green linear profiles. Pleural space cells and particles and or fibers (orange, if present) in contact with lung or pleura tissue are also shown.

Fig. 11, Panel 1 shows a typical image of an air control animal at day 45. The intercostal muscle, which runs between the ribs and is mainly involved in the mechanical aspect of breathing is seen on the left, adjacent to the parietal pleura. Just below the surface of the parietal pleura are the submesotheIial lymphatic lacunae into, which the pleural fluid flows through the stomata. The pressure oscillations in the lacunae, related either to tissue motion or contractile properties of myogenic cells, represent the main mechanism for lymph propulsion toward larger lymphatic collecting ducts (Negrini et al., 1992). The normal collagen of the visceral pleural is seen as a solid light green band.

High dose brake dust, Group 4 (Fig. 11, Panel 2) shows a similar image to the air control (note the chestwall is on the right of the image). A few particles with macrophages are present in the adjacent alveoli. For the TiO_2 particle control group (Fig. 11, Panel 3) a few particles are also noted in the lung as well as in the pleural cavity. In the chrysotile high dose Group 7, a few chrysotile particles are also seen in the pleural cavity (Fig. 11, Panel 4).

In the crocidolite exposed group 8 (Fig. 11, Panel 5), longer crocidolite fibers are present in the pleural space with a pronounced inflammatory response below the visceral pleura. In group 9 (Fig. 11, Panel 6), amosite asbestos, amosite fibers are directly below the visceral

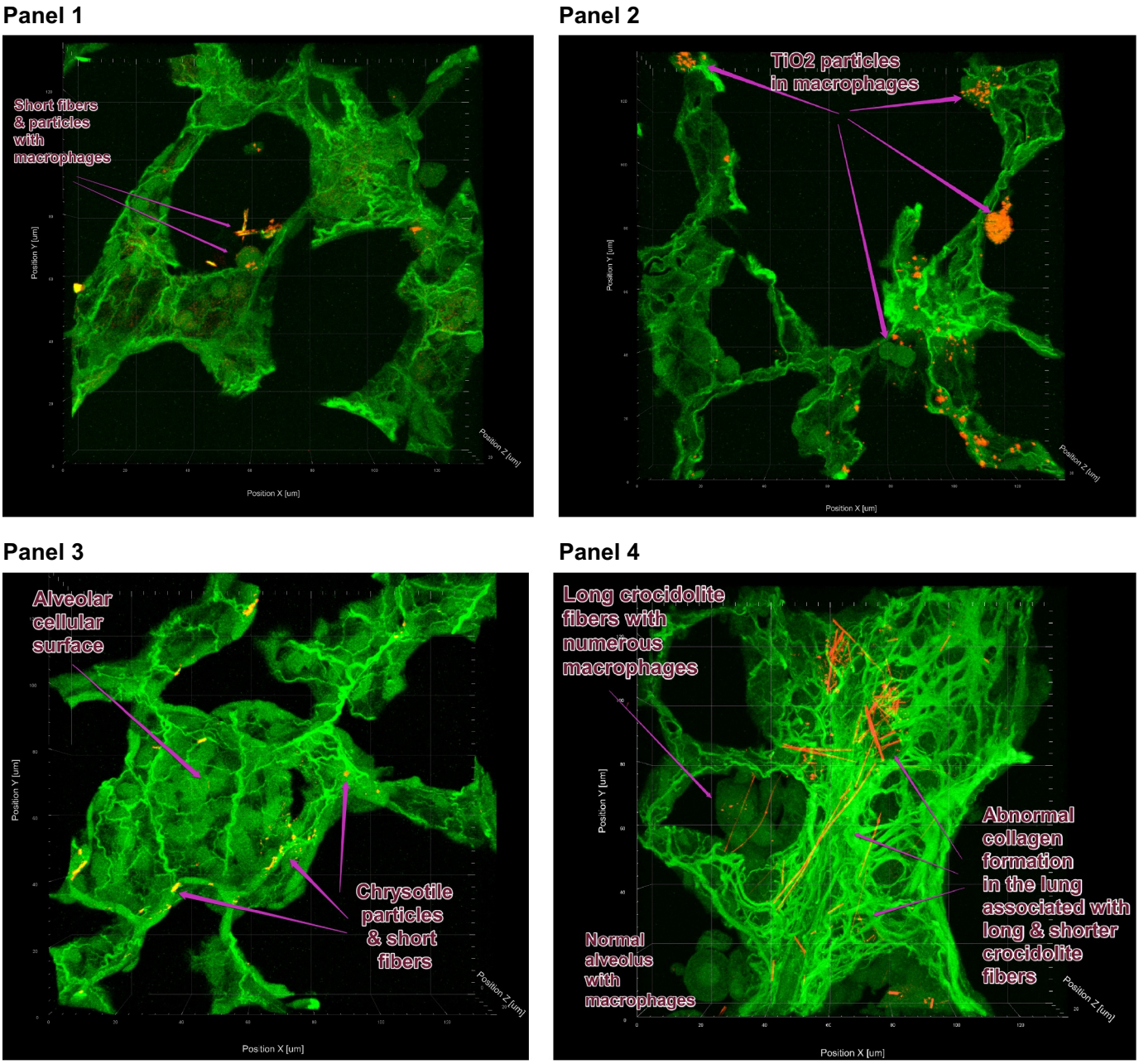

Fig. 9. Confocal images of the lung at 89 days. Bright green structures are connective tissue cables highlighted using maximum intensity projection from original image data. Particles and fibers are shown in orange. When protein coated, they appear yellow. These images are from projected three-dimensional reconstructions. The scale bars are in μm and are shown in each image in the surrounding frames.
Panel 1: Group 3, at 89 days: Normal Parenchyma, alveolar entrance. Short fibers are present with and without alveolar macrophages.
Panel 2: Group 5, TiO_2 at 89 days: Normal Parenchyma, alveolar entrance. TiO_2 particles are present in alveolar macrophages.
Panel 3: Group 7, chrysotile high dose at 89 days. Normal parenchyma showing an alveolus with cellular surface. Protein coated chrysotile particles and short fibers are present.
Panel 4: Group 8, Crocidolite at 89 days. Right: Conducting airway with localized connective tissue response within interstitial spaces. Left: Alveolus with long crocidolite fibers encapsulated in granuloma.
Panel 5: Group 9, Amosite at 89 days. Lung parenchyma with localized connective tissue response. Alveoli with long amosite fibers encapsulated in giant cells / microgranuloma. Blood vessel upper right of image surrounded by distal lymphatics with amosite particles/short fibers. (For interpretation of the references to colour in this figure legend, the reader is referred to the web version of this article.)

pleura, which is also associated with an inflammatory response. The collagen matrix of the parietal pleura appears much thicker as well.

At the end of exposure (89 days), the images from the air control, brake dust, TiO_2 and chrysotile groups show no significant differences from the 45 day time point.

In Group 8, crocidolite asbestos at 89 days (Fig. 12, Panel 1), fibers are seen in the pleural space and penetrating from the lung through the visceral pleura. The visceral and parietal pleura have increased collagen.

Fig. 12, Panels 1 and 2 shows images from Groups 8 and 9, crocidolite and amosite asbestos at 89 days. In Fig. 12, Panel 1, crocidolite fibers (one ~ 50 μm in length) are seen penetrating the visceral pleura. On the middle right, a number of crocidolite fibers are seen in the pleura associated with a notable inflammatory response. In Fig. 12, Panel 2, numerous amosite fibers are seen in the sub-pleural alveoli adjacent to the

Panel 5

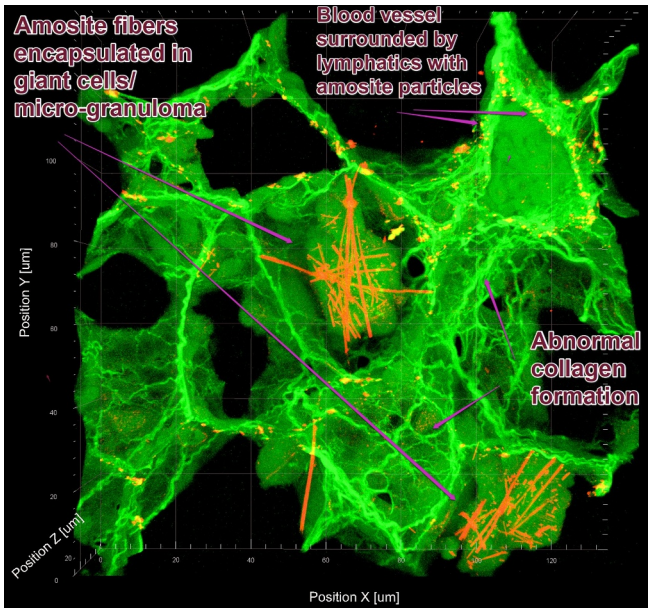

Fig. 9. (*continued*)

visceral pleura. In both Panels 1 and 2, an extensive collagen matrix has developed extending from the lung to the visceral pleura.

At 3 months post exposure (180 days), the images from the air control, brake dust, TiO_2 and chrysotile groups show no significant differences from the 45 and 89 day time points.

In Group 8, crocidolite asbestos at 180 days, Fig. 13, Panel 1 shows a long crocidolite fiber penetrating the visceral pleura. The sub-pleural alveoli exhibit an extensive inflammatory response. Fig. 13, Panel 2 shows for crocidolite an extensive inflammatory response with macrophages and neutrophils in the pleural space.

In Group 9, Fig. 13, Panels 3 & 4, amosite asbestos at 180 days, amosite fibers are present adjacent to the visceral pleura and associated with an inflammatory response. The visceral and parietal pleura have notably increased collagen thickness. In Fig. 13, Panel 4, the lacuna of the parietal pleura appears swollen. Activated mesothelial cells are present on the visceral and parietal pleura. A giant cell is present in the pleural space.

4. Discussion

This 90 day repeated dose inhalation toxicology study clearly shows that brake dust from brakes that use chrysotile in the matrix, produced no inflammatory response at exposure concentrations that were orders of magnitude greater than those reported for worker exposure (Part 1, Bernstein et al., 2019).

This is the first long-term inhalation toxicology study of brake dust with control groups of TiO_2, chrysotile and amphibole asbestos, crocidolite and amosite, that has been performed at exposure concentrations within a few orders of magnitude of human exposures in the past. In addition, the chrysotile and amphibole asbestos exposures had equivalent fiber exposures with similar long fiber (> 20 μm) aerosol concentrations and were conducted without extensively grinding or milling the fibers, thus enabling a direct comparison between fiber types.

Integrating into the study the histopathological examination with the confocal microscopy has provided a very powerful means for evaluating the potential for these materials to produce pulmonary effects and for assessing possible mechanisms by, which fibers may or may not translocate to the pleural cavity and produce disease.

This study is also unique in that it demonstrates that when the fiber characteristics and inhalation exposures are to be taken into account correctly, the inhalation model is the most sensitive method for evaluating potential fiber toxicity.

The brake dust that was evaluated was obtained from automobile brakes that were manufactured using chrysotile as one of the components. The original friction material contained approximately 30% chrysotile (analyzed in accordance with EPA 600/R-93/116 see Perkins and Harvey (1993))[5] (Bernstein et al., 2018); Blau (2001) has reported that brakes typically contained between 30 and 70% asbestos. The high dose brake dust aerosols contained a mean of 1297 to 2120 total fibers/cm^3, however, of these, there were only between 2 and 7 WHO fibers/cm^3 (means) depending on exposure group. Rhee (1974) determined that the wear of asbestos friction materials is controlled by a pyrolysis mechanism at elevated temperatures (above 450 °F drum temperature) and by adhesive and abrasive mechanisms at low temperatures. The wear mechanisms of the brake drums appear to favor the production of very short (< 5 μm) chrysotile fibers. Fibers longer than 20 μm were even fewer, with means ranging between 0.2 and 0.5 fibers L > 20 μm)/cm^3. Assuming a minimum of 30% chrysotile in the brake pads, based on the gravimetric and WHO fiber concentration of the chrysotile exposure group, the WHO fibers in the brake dust aerosol were < 2% of the total brake dust mass.

The particle control TiO_2 was aerosolized at a similar gravimetric concentration as the high dose brake dust (0.67 vs 0.70 mg/m^3). The aerosol concentrations from the two chrysotile aerosol exposure groups were 119 and 233 WHO f/cm^3 and 28 and 72 fibers(L > 20 μm)/cm^3, respectively. The crocidolite and amosite asbestos exposures were 181 and 281 WHO f/cm^3 and 24 and 48 fibers(L > 20 μm)/cm^3, respectively. Therefore, the fiber characteristics of the chrysotile, crocidolite and amosite aerosol were comparable.

The biosolubility/clearance of the brake dust plus chrysolite as compared to chrysotile and crocidolite asbestos alone has been reported by Bernstein et al. (2015a). The biosolubility of chrysotile results in accelerated clearance and lack of toxicity. This is also demonstrated in the present study through the absence of an inflammatory response, minimal tissue injury, and the low fibrogenic response. Chrysotile is a thin rolled sheet of magnesium on the outside and silica on the inside, which is acid soluble (Kobell, 1834; Whittaker, 1957; Whittaker, 1963; Tanji et al., 1984; Titulaer et al., 1993) explaining its biosolubility.

Amphibole asbestos fibers, such as crocidolite, are encased in silica and are insoluble at any pH that can occur in physiological conditions (Skinner et al., 1988; Whittaker, 1960). Those fibers, once deposited in the lung, which are too long to be cleared by the macrophage, persist in the lung and quickly initiate a sustained inflammatory response, leading to persistent tissue injury and a subsequent fibrogenic response.

4.1. Histopathological examination

The histopathological results reflect these differences in composition and structure of chrysotile versus amphibole asbestos and indicate that the response in the lung to the inhaled brake dust with chrysotile is what would be expected from a low dose insoluble particle exposure. That is, largely a macrophage response with the corresponding

[5] As reported by Blake et al. 2003, the asbestos-containing brake shoe was sampled and analyzed using polarized light microscopy according to the U.S. Environmental Protection Agency's Method 600 for the determination of asbestos in bulk building materials (Perkins and Harvey, 1993). The shoe was found to contain by area 30% chrysotile. Review of batch formulation data provided by the brake shoe manufacturer (AlliedSignal, Troy, MI) indicates the primary shoes contained 72% asbestos and the secondary shoes contained 50% by weight. Perkins and Harvey (1993) explain that the technique used, determined using polarized light microscopy the relative projected areas occupied by separate components in a microscope slide preparation of a sample. For asbestos analysis, this technique is used to determine the relative concentrations of asbestos minerals to nonasbestos sample components.

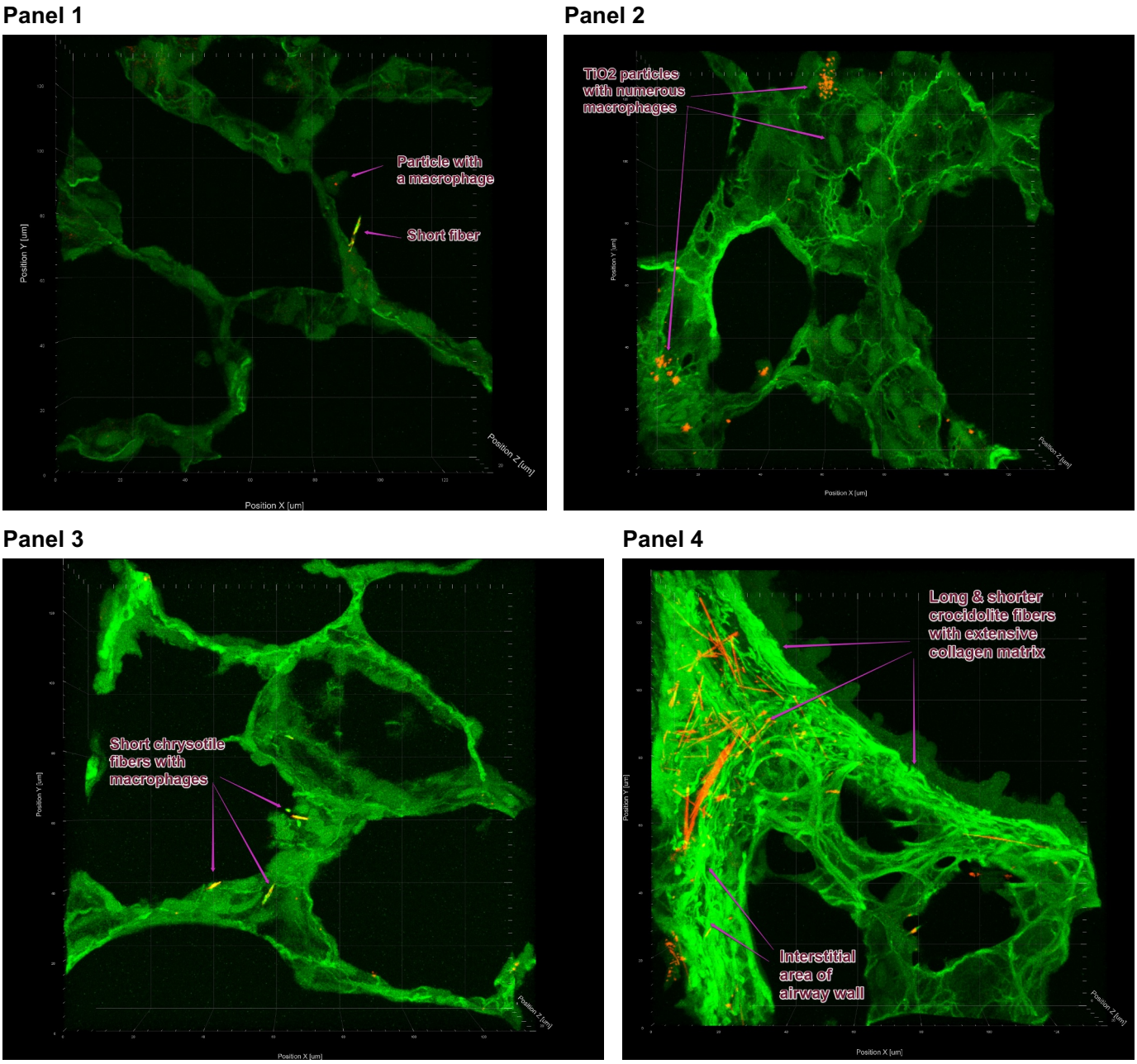

Fig. 10. Confocal images of the lung at 180 days. Bright green structures are connective tissue cables highlighted using maximum intensity projection from original image data. Particles and fibers are shown in orange. When protein coated they appear yellow. These images are from projected three dimensional reconstructions. The scale bars are in μm and are shown in each image in the surrounding frames.
Panel 1: Group 4, Brake dust high dose at 180 days: Normal parenchyma showing alveoli. A short fiber is present as well a macrophage with a particle/short fiber.
Panel 2: Group 5, TiO_2 particle control at 180 days: Normal Parenchyma with an alveolar duct. Present are macrophages some with TiO2 particles.
Panel 3: Group 7, chrysotile high dose at 180 days: Normal Parenchyma with an alveolar duct. A few short chrysotile fibers are present with macrophages.
Panel 4: Group 8, crocidolite asbestos at 180 days: Upper portion is a conducting airway with airway epithelium. Below is a matrix of activated Interstitial connective tissue with long & shorter crocidolite fibers.
Panel 5: Group 9, amosite asbestos at 180 days: On the left is a distal airway with amosite fibers penetrating and traversing the airway wall (center). Interstitial connective tissue with localized collagen response is present. On the right is a granuloma with numerous amosite fibers.
Panel 6: Group 9, amosite asbestos at 180 days: Distal airway with adjacent localized interstitial connective tissue response. In the center is a granuloma with long and shorter amosite fibers. Below left is an extensive collagen matrix with long and shorter amosite fibers. (For interpretation of the references to colour in this figure legend, the reader is referred to the web version of this article.)

accumulation of particle laden macrophages predominantly at bronchiolo-alveolar junctions. The response to the inhalation of brake dust exposure in the study was similar or less than that observed for TiO_2 an "poorly soluble, low toxicity" (PSLT) particle (Borm and Driscoll, 2019; ECETOC-TR-122, 2013).

In all of the brake dust exposed groups, there were few chrysotile fibers L > 20 μm remaining in the lungs at either 45 or 89 days (end of exposure). However, there were no fibers L > 20 μm remaining at 90 days post exposure (180 day time point).

To obtain comparative exposure concentrations for the chrysotile, crocidolite and amosite asbestos, intensive grinding or processing was avoided so as not to create excess particles and shorter fibers. For the

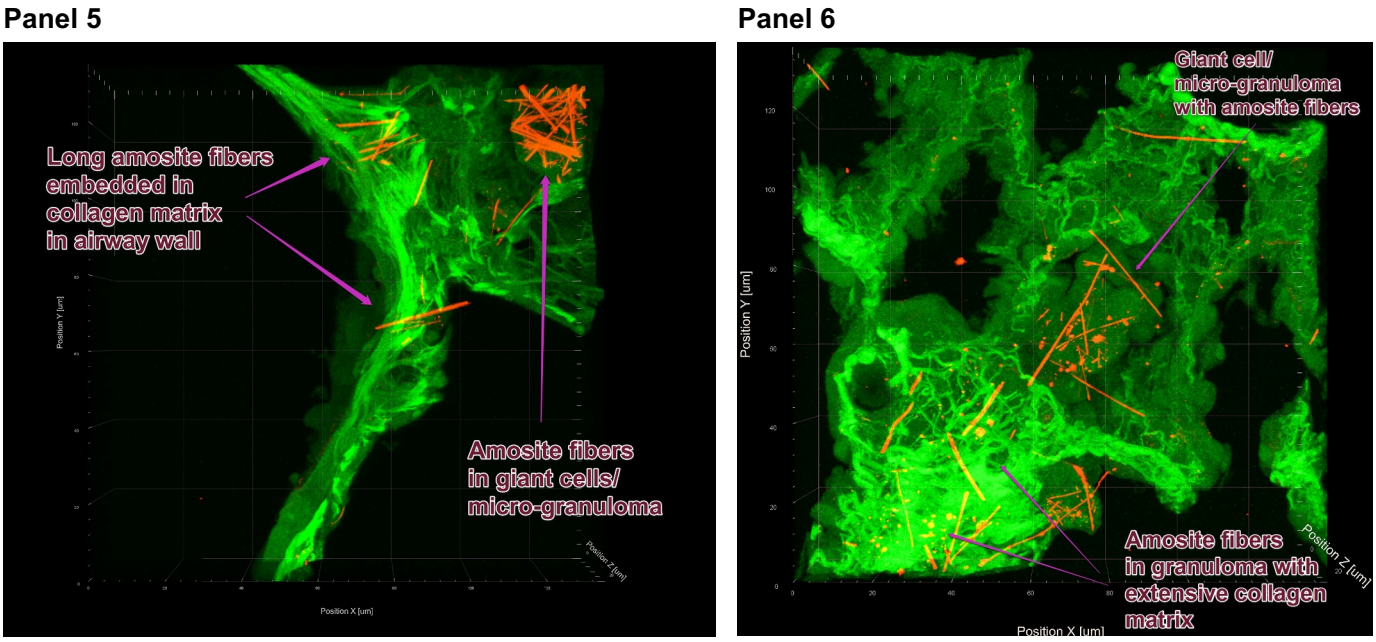

Fig. 10. (*continued*)

chrysotile, methods were developed, which opened the fiber bundles. For the crocidolite, the commercial fiber was so long that it was necessary to mill it briefly to assure that the fiber length would be rat respirable. As described Part I of the manuscript, the resulting bivariate length and diameter distributions of the chrysotile and crocidolite were very similar allowing in this study a direct comparison of the potential for producing a toxic response at a WHO fiber concentration ranging from 119 to 281 fibers/cm^3.

At the exposure concentrations used in the current study, the response to chrysotile in comparison to the amphibole asbestos crocidolite and amosite on a fiber for fiber basis is clearly differentiated.

The chrysotile exposures at 45 days resulted in (multi)focal very slight (minimal) alveolar/interstitial accumulation of particle-laden macrophages predominantly at bronchiole-alveolar junctions. Very slight (multi)focal occurrence of multinucleated (syncytial) giant cells was seen in a single rat of group 7 (Chrysotile high). At 89 and 180 days, accumulation of particle-laden macrophages predominantly at bronchiole-alveolar junctions was also observed. In the chrysotile high dose, very slight fibrosis was seen in two animals at 89 days only.

In comparison, at 45 day, the crocidolite and amosite asbestos exposure groups showed multifocal alveolar/interstitial accumulation of fiber-laden macrophages. (multi)focal peribronchial/peribronchiolar infiltration of mixed inflammatory cells were also observed in these groups as well as multifocal alveolar/interstitial (intraseptal) infiltration of mixed inflammatory cells. Multifocal very slight interstitial fibrosis was observed in all rats of group 8 (Crocidolite) and group 9 (Amosite) only. Similar but more severe findings were seen at 89 days, where the multifocal interstitial fibrosis was reported for group 8, Crocidolite (3 rats very slight, 1 rat slight) and group 9, Amosite (all rats slight). By 90 days post exposure (180 days), all rats in the amphibole groups were reported as having (multi)focal interstitial fibrosis (slight).

The Wagner scores (Fig. 2) clearly differentiate the response to crocidolite and amosite asbestos from that to the brake dust groups, TiO_2 as well as the chrysotile groups.

Confocal imaging and collagen quantification:

The inclusion of the confocal imaging and collagen quantification both in the lung and the pleural cavity provides a powerful addition to the conventional histopathological examination. The results from histopathological examination (Table S-2 and S-3, supplementary data) provide detailed analysis of the response in the lung as a result of the various exposures, which included the evaluation for the presence of interstitial fibrosis. The pathologist also performed a semi-qualitative quantification of the amount of fibrosis in the lung, using a grid of 100 μm × 100 μm size, which was overlaid on the tissue (each counted square was 10,000 μm^2 or 0.01 mm^2 in size). Squares were counted as positive if the changes within the square were consistent with the changes of a Wagner grade 4 or higher (early interstitial fibrosis or more) as shown in Table 2. Otherwise it was counted as negative. This provides a semi-quantitative assessment of the presence or absence of collagen in each of the squares, but not the total amount.

The confocal imaging of the lung and chestwall (pleural region), in addition to providing detailed imaging of the lung and chestwall, provides the ability to quantify the amount of collagen present in the lung parenchyma, visceral and parietal pleura.

The 3D confocal images were colour coded for tissues, macrophages and other inflammatory cells such as neutrophils in various hues of green, with connective tissue being presented as brightest green in colour. The intensity of the green images was directly proportional to the amount of collagen present. Test article, such as brake dust particles, titanium oxide particles, chrysotile fibers, crocidolite and amosite fibers are shown in orange. Well over 12,000 confocal micrographs were recorded from each animal to obtain the necessary quantitative information. For this aspect of the study, over 432,000 images were recorded per time point.

The confocal analysis fully supports the results from the histopathological examination and provides additional precision and quantification in the assessment of possible fibrotic response with the three-dimensional images elucidating the relationship of fiber type to disease and the translocation of fibers within the lung and to the pleural cavity. The confocal examination quantified as well, the presence and length of fibers. At day 45 this examination was conducted for the airway regions in addition to the lung parenchyma.

Over all of the fiber exposed groups (groups 6,7,8 & 9), 12% of the WHO fibers were found in the distal airways, the remainder being in the lung parenchyma. For the fibers longer than 20 μm, 8% were found in the airways. The largest number of fibers were found to be in the range of 5–20 μm. In this range, 8% of the chrysotile high dose, 8% of the crocidolite and 15% of the amosite were found in the airways. These results support that the exposure aerosols were largely rat respirable as

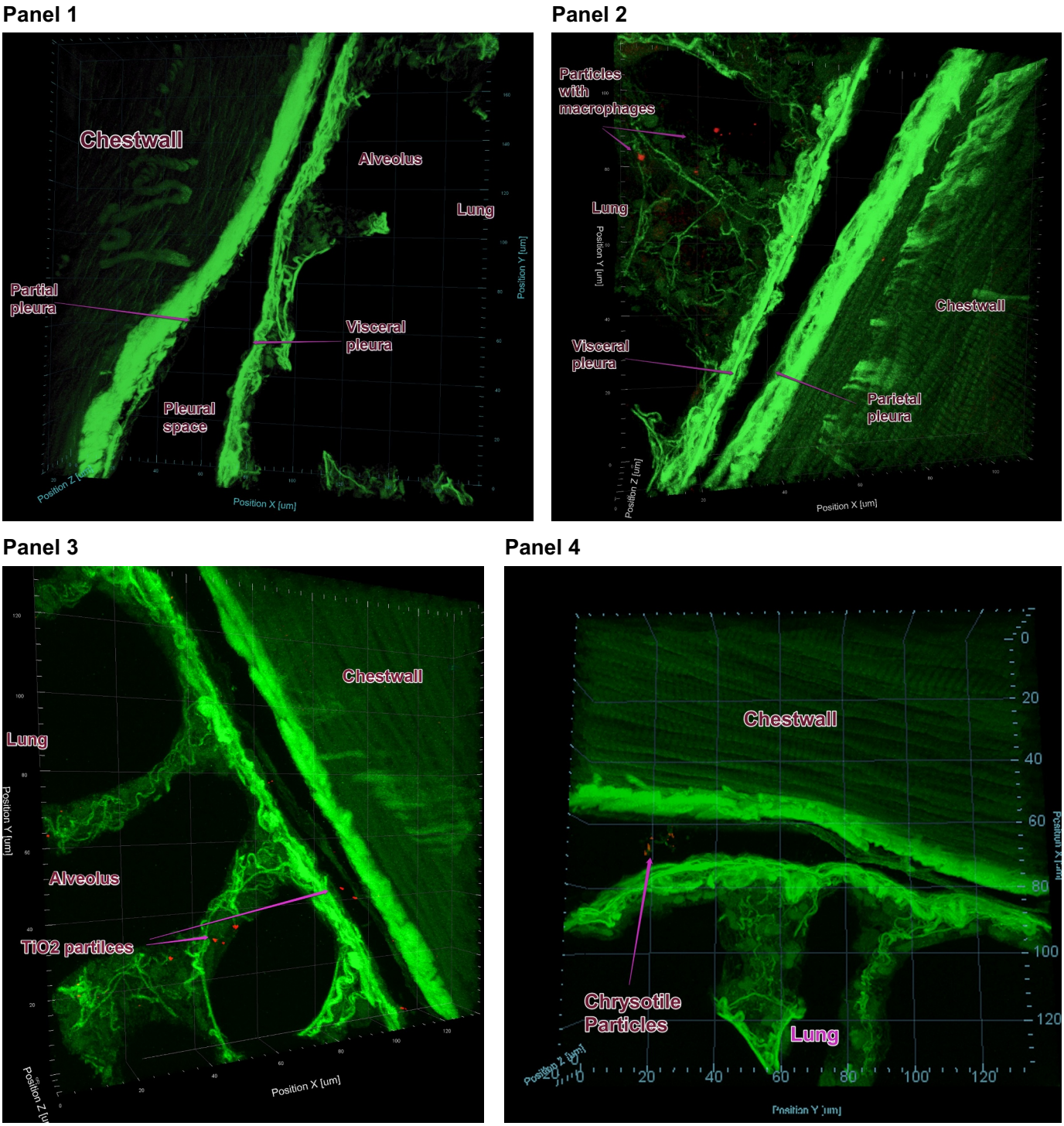

Fig. 11. Confocal images of the pleura at 45 days. Bright green structures are connective tissue cables highlighted using maximum intensity projection from original image data. Particles and fibers are shown in orange. When protein coated they appear yellow. These images are from projected three dimensional reconstructions. The scale bars are in μm and are shown in each image in the surrounding frames.
Panel 1: Group 1, Air control Pleura at 45 days
Panel 2: Group 4 High dose brake dust Pleura at 45 days
Panel 3: Group 5 TiO2 particle control Pleura at 45 days
Panel 4: Group 7 Chrysotile high dose Pleura at 45 days
Panel 5: Group 8 Crocidolite asbestos Pleura at 45 days
Panel 6: Group 9 Amosite asbestos Pleura at 45 days (For interpretation of the references to colour in this figure legend, the reader is referred to the web version of this article.)

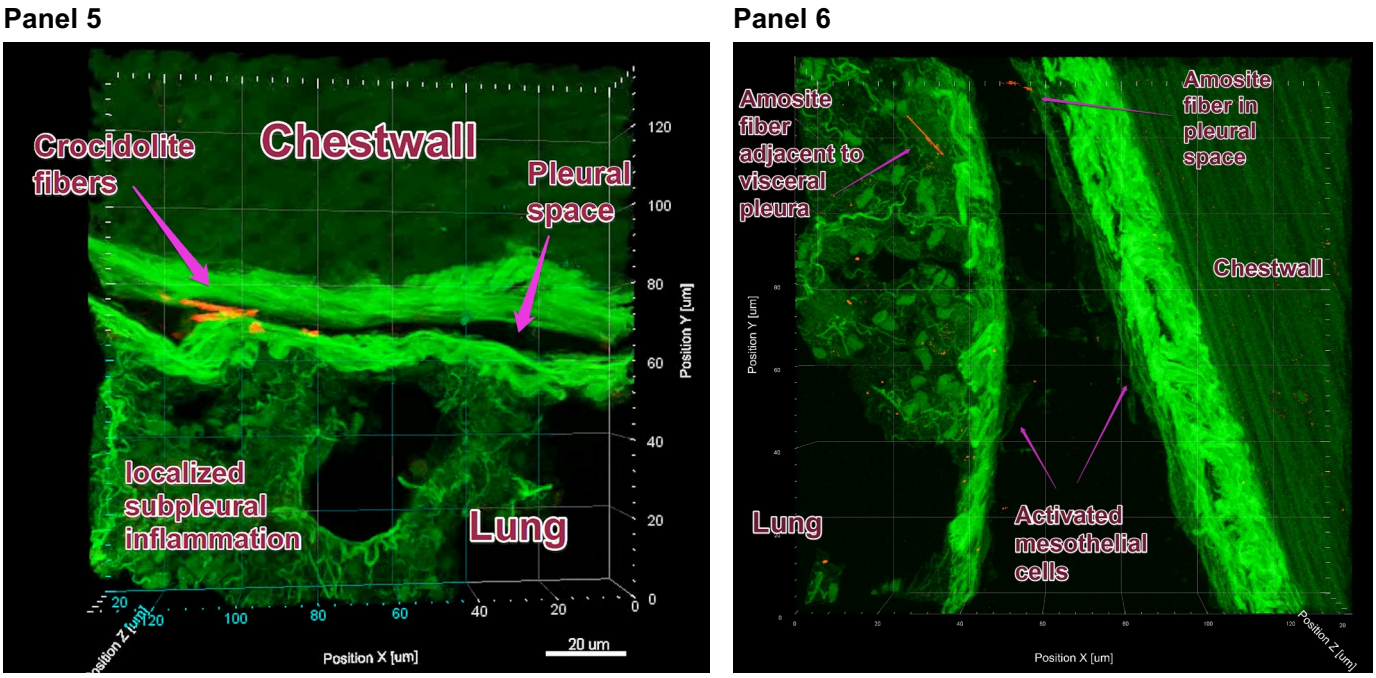

Fig. 11. (*continued*)

described in Part I of the manuscript.

In the brake dust groups, the particles and chrysotile fibers are seen either in macrophages or free in the lung alveoli. The free fibers are often coated with an organic proteinaceous layer, which appears as shades of yellow in the confocal images. This coating appears to signal that these fibers may not be bioactive as they often appear without macrophages or any other cells attracted to them.

The particles in the TiO_2 control group are uniform and are seen either phagocytized by macrophages or less often free in the alveoli. The TiO_2 particles are insoluble in dilute alkali or dilute acid and as seen in the confocal images tend to accumulate in the macrophages. Considerably fewer brake dust particles are seen in the lung or macrophages, which suggests that the brake dust particles are more soluble either in the lung surfactant (neutral pH) or the macrophage vacuoles

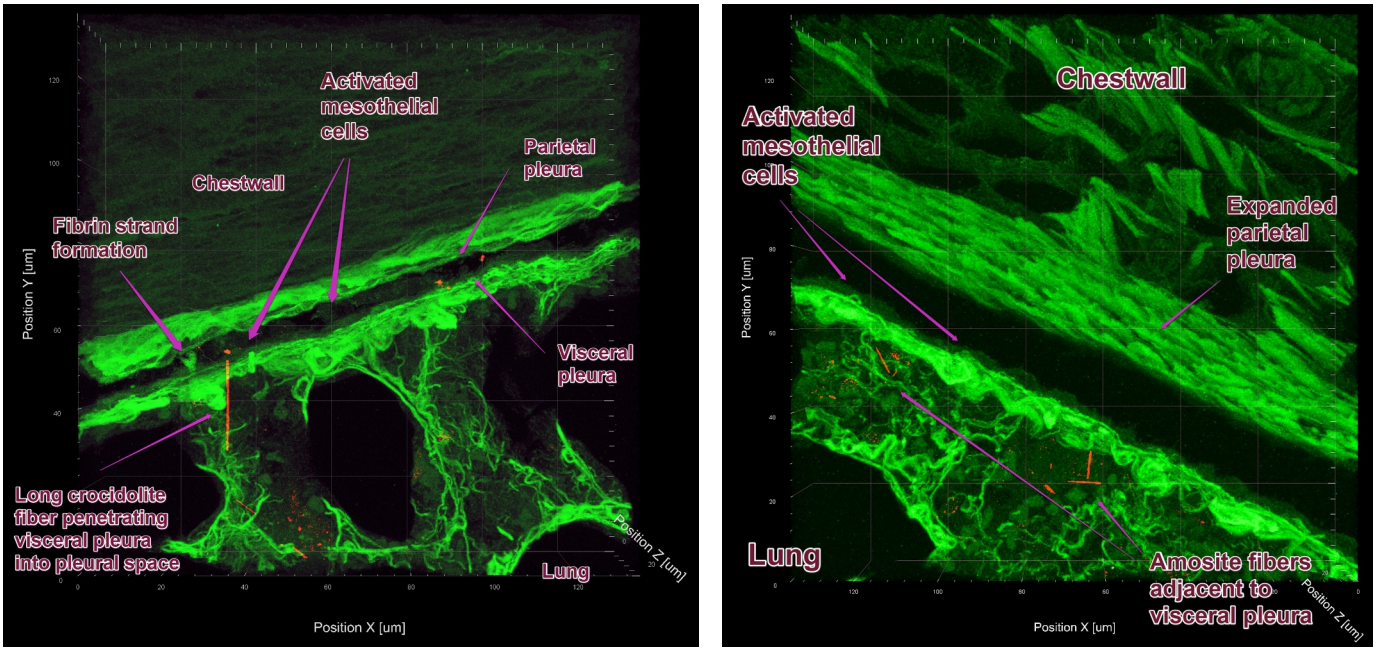

Fig. 12. Confocal images of the pleura at 89 days. Bright green structures are connective tissue cables highlighted using maximum intensity projection from original image data. Particles and fibers are shown in orange. When protein coated they appear yellow. These images are from projected three dimensional reconstructions. The scale bars are in μm and are shown in each image in the surrounding frames.
Panel 1: Crocidolite Group 8 at 89 days
Panel 2: Amosite Group 9 at 89 days (For interpretation of the references to colour in this figure legend, the reader is referred to the web version of this article.)

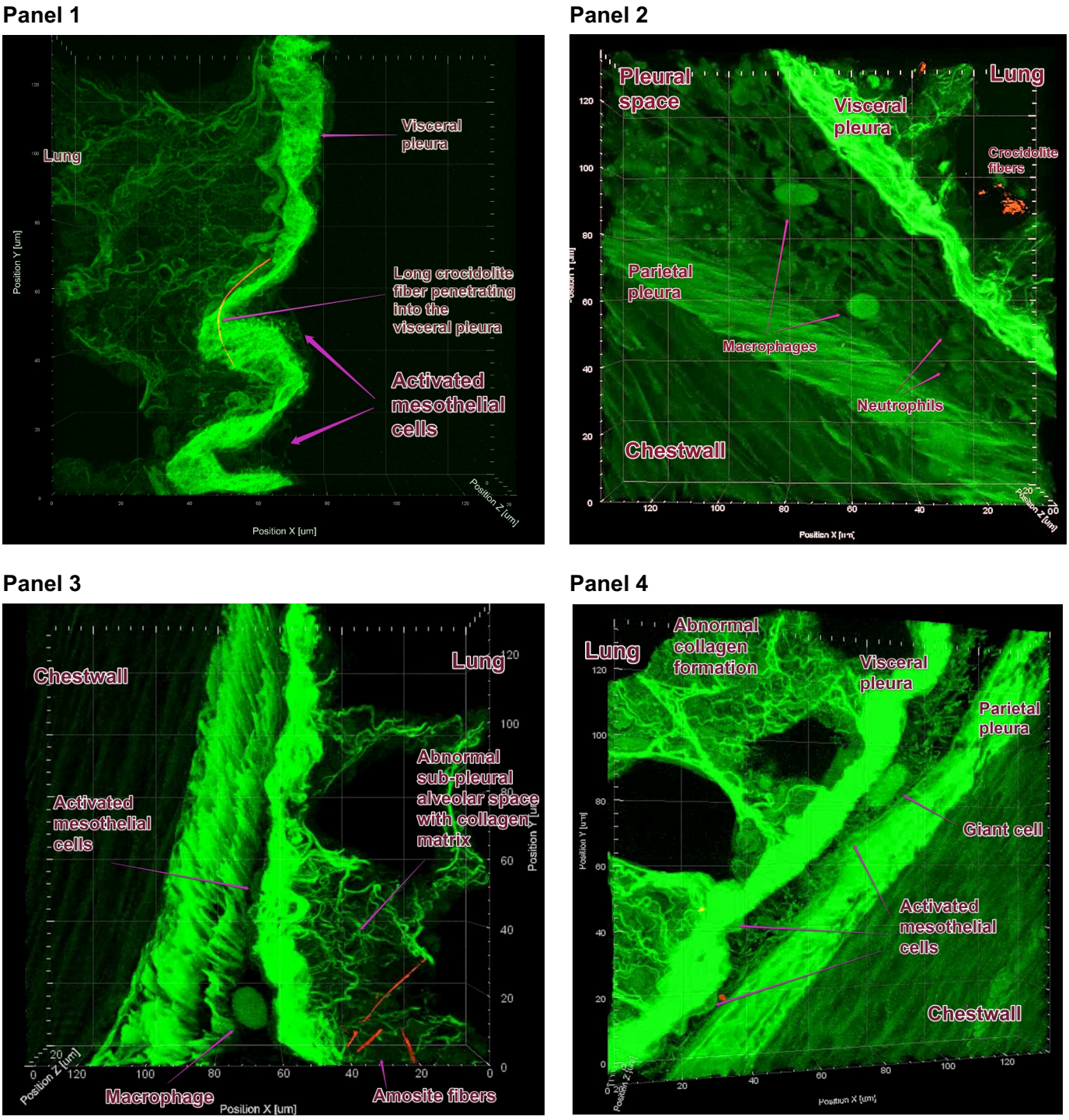

Fig. 13. Confocal images of the pleura at 180 days. Bright green structures are connective tissue cables highlighted using maximum intensity projection from original image data. Particles and fibers are shown in orange. When protein coated they appear yellow. These images are from projected three dimensional reconstructions. The scale bars are in μm and are shown in each image in the surrounding frames.
Panel 1: Crocidolite asbestos – Group 8 at 180 days
Panel 2: Crocidolite asbestos – Group 8 at 180 days
Panel 3: Amosite asbestos – Group 9 at 180 days
Panel 4: Amosite asbestos – Group 9 at 180 days (For interpretation of the references to colour in this figure legend, the reader is referred to the web version of this article.)

(acid pH).

In the low and high dose chrysotile exposure groups, the WHO fiber aerosol exposures are 18 and 35 times that in the high dose brake dust group. While considerably more fibers longer than 20 μm are present in the chrysotile aerosol, few are observed in the lung by the confocal examination. Poland (2019) describes the chemical structure of chrysotile and leaching mechanisms following inhalation, which leads to dissolution and fragmentation. (I) Deposition of chrysotile fibers in the lung environment. (II) Longitudinal splitting of the fiber into thinner fibrils. (III) Leaching of magnesium from the brucitic layer resulting in

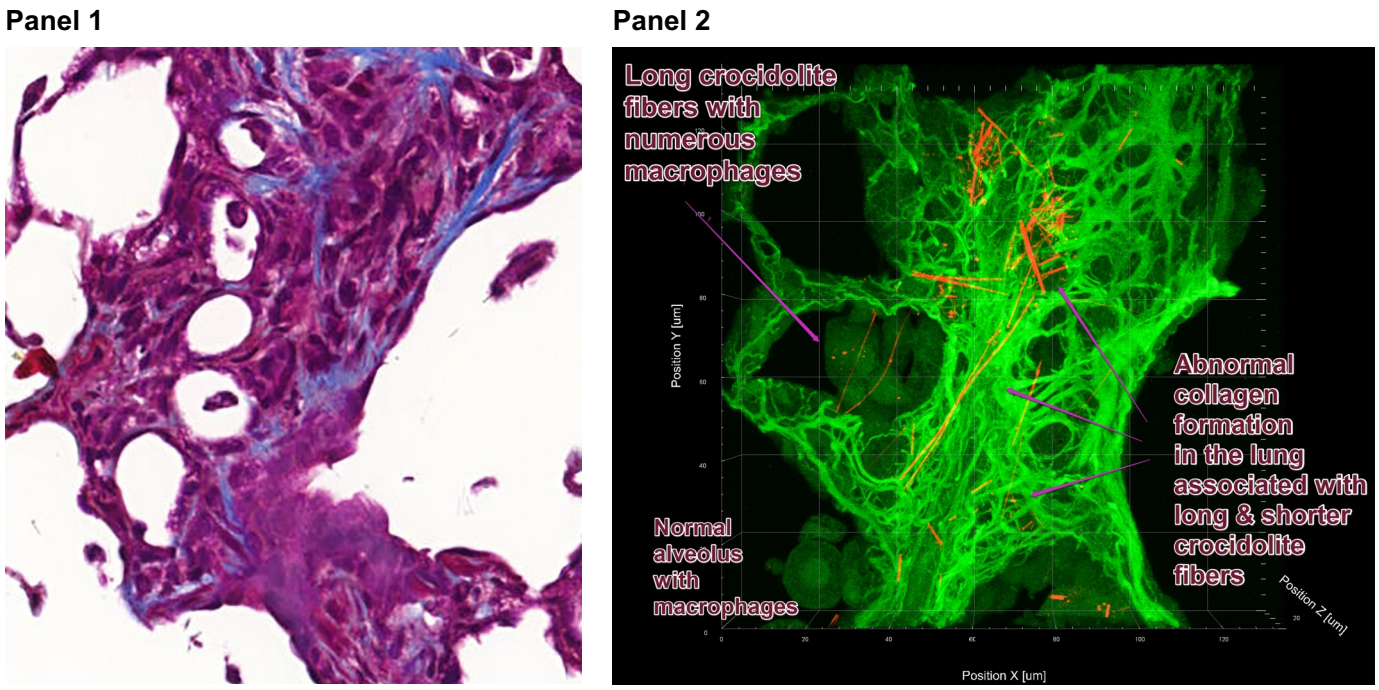

Fig. 14. Left histopathological image from Group 8, 89 days showing a focal slight (*fibrosis*) microgranuloma in the lung: Wagner Grade 4 : 79/7554 = 1.05%. Right: Confocal micrograph from Group 8, 89 days showing a similar lesion
Panel 1: Histopathological image from Group 8, 89 days (Figure *47 8013_29_MT_x20*).
Panel 2: Confocal micrograph from Group 8, 89 days (Fig. 9, Panel 4: Group 8, Crocidolite at 89 days.

the formation of a weakened metastable pseudomorph formed of the remaining silica structure. (IV) Transverse breakage of the weakened silica structure into short fragments. In Fig. 7, Panel 5 (Group 7) chrysotile fibers appear to have undergone this last step and have broken apart following inhalation.

The contrast between the brake dust with chrysotile groups and the chrysotile alone groups to what is observed and measured in the amphibole asbestos groups of crocidolite and amosite is notable. The presence of numerous longer fibers and the associated intensity of the pulmonary responses as shown in Figs. 7, Panels 6–8; Fig. 8, Panels 4 & 5, respectively, contrasts with normal macrophage particulate clearance of insoluble particles as described by Oberdoerster, 1993 and Riediker et al. (2019) observed in the brake dust, TiO_2 and chrysotile exposure groups. As shown in Fig. 8, Panel 5 (amosite asbestos at 89 days), the long amosite fibers are not cleared and create a significant pathological response with enhanced collagen formation. In the same panel, the amosite particles and short fibers can be seen in the lymphatics, which surround the blood vessel and alveoli as described by Cloutier and Thrall (2009).

The correspondence of the histopathological examination with the confocal microscopy is illustrated in Fig. 14. On the left is a histopathological image from Group 8, 89 days showing a focal slight microgranuloma in a lung that was scored as Wagner Grade 4. The Masson trichrome stain used in this image shows the fibrosis as blue/purple bands (the fibers are not clearly observed). On the right is a 3D confocal image showing a similar microgranuloma lesion from Group 8, 89 days. The crocidolite fibers present in the lesion are clearly shown in orange. The fibrotic collagen network that has developed is shown as the bright green strands throughout the lesion. In the alveoli, long crocidolite fibers can be seen with groups of macrophages and giant cells. The confocal image shows as well that the collagen matrix is much more extensive than can be appreciated from the histopathological image.

The histopathology and confocal examination clearly differentiate the response of brake dust, TiO_2 and chrysotile from that of the amphibole asbestos crocidolite and amosite in the lung. It confirms that the amphibole fibers initiate a pathological response early on which persists and continues the development of this response in stark contrast to brake dust, TiO_2 and chrysotile.

4.2. Confocal chestwall examination

While the response of these exposures in the lung is important, the target area that is unique to fibers is the pleural cavity.

The analysis of the snap frozen chestwall presented in this study provides a highly sensitive method of assessing the pleural response to fibers and the development of lesions on both the visceral and parietal pleura, which would otherwise be undetected by the conventional histopathological examination.

The fluid dynamics of the lung and pleural cavity dictates the use the snap frozen chestwalls for the assessment of fiber translocation and pathology in the pleural cavity. In vivo, there exists an extensive dynamic balance of fluid and air pressures within the lung, the lymphatic system and the pleural cavity (Breslin et al., 2019). The lymphatic system, which is active in clearing short fibers and particles, has a unique system of one-way valves, which maintains the lymph flow in the correct direction (Moore and Bertram, 2018; Scallan et al., 2016). At conventional necropsy, these physiological restraints are no longer active and the lymphatic and lung fluids and fibers can drain into the pleural cavity. The snap frozen chestwall procedure used in this study captures the momentary condition of the pleural cavity without such artifacts.

In the previous 28 days study (Bernstein et al., 2018), the quantification of the mesothelial thickness was found to be a sensitive indicator of the initiation of pleural pathological response following crocidolite asbestos exposure with approximately double the visceral and parietal mesothelial thickness as compared to the air control, brake dust or chrysotile exposed groups. In the current 90 days study the exposure used similar cumulative doses as were used in the 28-day study but spread out over 13 weeks, that is the exposure concentrations were correspondingly lower in the 90-day study as compared to the 28-

day study.

While confocal images of the pleural cavity have identified activated mesothelial cells on the visceral pleura in crocidolite and amosite exposed rats (e.g. Fig. 11, Panels 1 & 2 and Fig. 12), at these lower exposure concentrations, through 90 days post-exposure (180 days), there are no statistically significant differences in mesothelial thickness between groups. The ANOVA and Dunnett's analysis are presented in Section S-6 (Supplemental data). These lower aerosol concentrations more closely correspond (although still orders of magnitude greater) to exposures that have been reported for humans. As with humans exposed to amphiboles, the progression of the animals to pleural disease is relatively slow. The subsequent observations at sacrifice time points through the animal's life time will be examined for evolution that is suggested already in these early time points.

The confocal imaging of the visceral and parietal pleura provides further evidence of the marked contrast in pleural response of brake dust, TiO_2 or chrysotile exposure compared to that from crocidolite or amosite asbestos. Fig. 10, Panels 1–4 shows confocal images from the air control, brake dust, TiO_2 and chrysotile exposed animals at 45 days. What is seen is a particulate response with occasional particles seen in the lung and the pleural cavity, a normal clearance pathway for lung particulates. No fibers were observed in the pleural space.

Fig. 10, panel 5 shows a large granulomatous response in the lung and approximately 20 μm crocidolite fibers in the pleural cavity at 45 days. The amosite exposure (Panel 6) at 45 days shows the presence of long sub-visceral pleura fibers, a fiber in the pleural space and activated mesothelial cells on both the visceral and parietal pleura.

At 89 days, a long crocidolite fiber is seen penetrating the visceral pleura (Fig. 11, panel 1) with activated mesothelial cells present on both the visceral and parietal pleura.[6] In the region of fiber penetration into the pleura and adjacent to it are fibrin strands. Jantz and Antony (2006) have described these events as part of the mechanism in the formation of pleural fibrosis. Fig. 11, panel 2, shows the pleural region from an amosite exposed rat at 89 days. Several amosite fibers are present in the lung adjacent to the visceral pleura with a dense inflammatory matrix and activated mesothelial cells along the length of the visceral pleura. In addition, the parietal pleura appears with the lacuna expanded likely as a result of increased pleural fluid.

Fig. 12, Panels 1 & 2 show the pleural region from crocidolite exposed rats at 90 days post exposure (180 days). In Panel 1, a long crocidolite fiber is seen penetrating the visceral pleura, which shows increased collagen formation (bright green band) and activated mesothelial cells. In Panel 2, an extensive response to the fibers is present on the visceral and parietal pleura and within the pleural space where macrophages and neutrophils are present in a dense matrix of pleural fluid and fibrin strands.

In Panels 3 & 4 (Fig. 12) amosite asbestos exposure is seen to also produce a continued pleural response at 180 days. Long amosite fibers are present adjacent in the sub-visceral pleura region surrounded by a collagen matrix with activated mesothelial cells lining the visceral and parietal pleural surfaces. The visceral pleura has thickened collagen formation and the parietal pleura appears swollen, likely from fluid created by the inflammatory response to the fibers.

Rat model sensitivity:

The dose response results of this 90 day sub-chronic inhalation toxicology study support the sensitivity of the inhalation route when performed correctly. As this animal model has evolved over time from installation to exposure extremes in which there is an overload of the lung, this study has demonstrated that at exposures within orders of magnitude of human exposures that fiber toxicity can be clearly demonstrated in a well-controlled animal study.

In most early studies, there was little characterization of the fibers and exposure was most often based upon equivalent gravimetric concentrations (10 mg/m^3 with > 100,000 WHO f/cm^3) rather than equivalent fiber number and length (Bernstein, 2015. In this study, the mean chrysotile aerosol exposure concentrations were 119 and 233 fibers(WHO)/cm^3 (0.27 and 0. 64 mg/m^3, respectively). The chrysotile fiber exposure concentration in this study was 2975 to 5825 times the mean historical brake dust exposure TWA and 50 to 175 times the levels used in the brake dust exposed groups. Even at these concentrations, the response to chrysotile is largely that of an insoluble dust. At comparative exposure concentrations of 181 and 281 fibers(WHO)/cm^3 (1.28 and 2.32 mg/m^3, respectively), the crocidolite and amosite amphibole asbestos produced an array of fiber related pathological responses including interstitial fibrosis and pleural mesothelial activation, which persisted following the termination of exposure.

The sensitivity of the rat inhalation model for assessing fiber toxicology has been discussed extensively (Pott, 1991; Brown, 1991; McClellan et al., 1992). Pott (1989) concluded that the inhalation model was not sensitive and proposed using the intraperitoneal injection model to assess fiber toxicity. His reasoning was based upon many asbestos fiber inhalation studies of that era, which did not fully understand the importance of fiber diameter and length and how to aerosolize fibers without extensive breakage. McClellan based largely on a series of chronic inhalation studies of MMMF (man made mineral fibers) (Table 11.3, Bernstein, 2006) that the fiber inhalation model was the most sensitive and the natural route of exposure. Brown et al. (1991) reported in the section “Discussion of the Proposal for the Classification of Fibres” that McClellan stated that “If positive results are obtained in an inhalation exposure bioassay using very high fiber exposure concentrations, I suggest the material be identified as ‘possibly carcinogenic to humans’.” while Pott advocated “In relation to human exposure, a concentration of a few hundred fibres/ml has to be evaluated as very high”.

The current studies combine both Dr. McClellan's and Dr. Pott's concepts confirming at concentrations of a few hundred fibers/ml results from earlier higher dose rat inhalation toxicology studies with amphiboles (Table 11.3, Bernstein, 2006).

5. Conclusions

The interim results from this 90 day multi-dose, inhalation toxicology study with life-time post-exposure observation have shown an important fundamental difference in persistence and pathological response in the lung between brake dust derived from brake pads manufactured with chrysotile or chrysotile alone in comparison to the amphiboles, crocidolite and amosite asbestos.

The use of imaging and quantitative confocal microscopy as a complement to classical histopathological examination and bronchoalveolar lavage provides enhanced definition and understanding of the response in the lung and the pleural cavity to brake dust with chrysotile as compared to TiO_2, chrysotile alone or crocidolite or amosite.

In the brake dust containing chrysotile exposure groups no significant pathological responses were observed at any time at exposure concentrations well above those at, which humans have been exposed. In response to high brake dust exposure levels in the test atmospheres slight accumulation of particles laden macrophages was noted. This was reflected by non-dose dependent Wagner scores, which ranged from 1 to 2 (with one being the level in the air control group). Similar scores were observed for the TiO_2 exposed group.

Chrysotile is not biopersistent, resulting in weakening of its matrix and breakage into short fibers & particles that can be cleared by alveolar macrophage clearance and continued dissolution. In the two

[6] Individual pleural mesothelial cells are linked together into a tight membrane by connecting intracellular proteins at key areas called adherens junctions. Activation of the pleural mesothelial monolayer by malignant cells, bacteria, or cytokines causes a breach in the integrity of the pleura and results in altered shape and gap formation between mesothelial cells, leakage of protein and fluids, and movement of phagocytic cells into the pleural space (Jantz and Antony, 2006).

chrysotile exposure groups, particle laden macrophage accumulation was noted leading to a slight interstitial inflammatory response (Wagner score 1–3). There was no peribronchiolar inflammation and occasional very slight interstitial fibrosis.

Both crocidolite and amosite asbestos induced elevated neutrophils (BAL), persistent inflammation, microgranulomas, and fibrosis (Wagner score 4), which persisted through the post exposure period. The confocal microscopy of the lung and snap frozen chestwalls also clearly differentiated the amphibole asbestos, which resulted in extensive inflammatory response, and collagen development in the lung and on the visceral and parietal surfaces.

This study is also unique in that it demonstrates that when the fiber characteristics and inhalation exposure are taken into account correctly, that the inhalation model is the most sensitive method for evaluating potential fiber toxicity.

The results reported here, provide already a clear basis for differentiating brake dust exposure from the effects following amphibole asbestos exposure. The subsequent results through life-time post-exposure will follow in later papers.

Declaration of competing interest

This study was funded by Honeywell International Inc. All protocol, design of the experimental procedures and the choice of laboratories was performed by D.M. Bernstein inconjunction with the scientific advisory board (see acknowledgements, below). The laboratory work to Citoxlab, Fraunhofer Institute, GSA and Rogers Imaging was sub-contracted by D.M. Bernstein. The affiliations of the authors are as shown on the cover page and include research laboratories, government institute, corporate affiliations, as well as independent toxicology consultant. This publication is the professional work product of the authors and may not necessarily represent the views of the corporate sponsor. One of the authors, David Bernstein, has appeared as an expert witness in litigation concerned with alleged health effects of exposure to chrysotile. Honeywell is a defendant in asbestos-product litigation and its predecessor manufactured the automotive brakes used in this study. There have been periodic communications between Honeywell and the authors concerning the status of this study. The contribution of Prof JI Phillips is based on research supported by the National Research Foundation.

Acknowledgements

The authors wish to acknowledge the excellent contribution to the design and conduct of this study of Drs. Vincent Castranova, Annie M. Jarabek, Ernest E. McConnell and Günter Oberdörster who served as members of an independent scientific advisory board to this study. We also wish to acknowledge the excellent work of the inhalation technical group staff at CiToxLab: András Bálint, Zoltán Jónás, Imre Bíró, Huba Szabó, Dániel Zentai-Papp, Zoltán Németh, Dániel Németh, László Ács and the necropsy group members: Ferenc Szűcs, Henrietta Miklós, Hajnalka Lovasi, István Róka in the performance of this study. We would also like to thank Stephane Gaering for his expertise and technical assistance.

Appendix A. Supplementary data

Supplementary data to this article can be found online at https://doi.org/10.1016/j.taap.2019.114847.

References

Bernstein, D.M., 2006. Fiber toxicology chapter. In: Gardner, D.E. (Ed.), Toxicology of the Lung, 4th edition. CRC Press/Taylor & Francis Group, Boca Raton, FL (0-8493-2835-7).
Bernstein, D., Salem, H., Katz, S., 2015. Serpentine and Amphibole Asbestos, Chapter 14. Inhalation Toxicology. CRC Press, Taylor & Francis, Boca Raton, FL, pp. 295–326.
Bernstein, D.M., Rogers, R., Sepulveda, R., Kunzendorf, P., Bellmann, B., Ernst, H., Phillips, J.I., 2014. Evaluation of the deposition, translocation and pathological response of brake dust with and without added chrysotile in comparison to crocidolite asbestos following short-term inhalation: interim results. Toxicol. Appl. Pharmacol. 276 (1), 28–46.
Bernstein, D.M., Rogers, R., Sepulveda, R., Kunzendorf, P., Bellmann, B., Ernst, H., Creutzenberg, O., Phillips, J., 2015. Evaluation of the fate and pathological response in the lung and pleura of brake dust alone and in combination with added chrysotile compared to crocidolite asbestos following short-term inhalation exposure. Toxicol. Appl. Pharmacol. 283, 20–34.
Bernstein, D.M., Toth, B., Rogers, R., Sepulveda, R., Kunzendorf Phillips, J., Ernst, H., 2018. Evaluation of the dose-response and fate in the lung and pleura of chrysotile-containing brake dust compared to chrysotile or crocidolite asbestos in a 28-day quantitative inhalation toxicology study will be published. Toxicol. Appl. Pharmacol. Vol 351, 74–92.
Bernstein, D.M., Toth, B., Rogers, R.A., Kling, D., Kunzendorf, P., Phillips, J.I., Ernst, H., 2019. Evaluation of the exposure, dose-response and fate in the lung and pleura of chrysotile-containing brake dust compared to TiO2, chrysotile, crocidolite or amosite asbestos in a 90-day quantitative inhalation toxicology study – interim results Part 1: Experimental design, Aerosol exposure, Lung burdens and BAL. Toxicol. Appl. Pharmacol.
Blau, P.J., 2001. Compositions, Functions, and Testing of Friction Brake Materials and Their Additives. Prepared by OAK RIDGE NATIONAL LABORATORY Oak Ridge, Tennessee 37831-6285. Prepared for U.S. Department of Energy, Assistant Secretary, for Energy Efficiency and Renewable Energy, Office of Transportation Technologies, August 2001. ORNL/TM-2001/64.
Borm, P.J.A., Driscoll, K.E., 2019. The hazards and risks of inhaled poorly soluble particles - where do we stand after 30 years of research? Part. Fibre Toxicol 16 (1), 11.
Breslin, J.W., Yang, Y., Scallan, J.P., Sweat, R.S., Adderley, S.P., Murfee, W.L., 2019. 2019 Lymphatic Vessel Network Structure and Physiology. Compr Physiol 9, 207–299.
Brown, 1991. Section 6 Discussion of the Proposal for the Classification of Fibres. In: Brown, C.R., Hoskins, J.A., Johnson, N.F. (Eds.), Mechanisms in Fibre Carcinogenesis. Plenum Press, New York and London, pp. 562–563.
Cloutier, M.M., Thrall, R.S., 2009. The respiratory system. In: Koeppen, B.M., Stanton, B.A. (Eds.), Berne & Levy Physiology, 6th ed. Mosby Elsevier, Philadelphia, PA, pp. 415–484.
ECETOC-TR-122, 2013. Poorly Soluble Particles/Lung Overload. Technical Report No. 122. European Centre for Ecotoxicology and Toxicology of Chemicals, 2 Avenue E. Van Nieuwenhuyse (Bte 8), B-1160 Brussels, Belgium.
EPA 712–C–98–204, 1998. Health Effects Test Guidelines OPPTS 870.3465 90-Day Inhalation Toxicity. United States Environmental Protection Agency August. https://www.regulations.gov/document?D=EPA-HQ-OPPT-2009-0156-0014.
Jantz, M.A., Antony, V.B., 2006. Pleural fibrosis. Clin. Chest Med. 27 (2), 181–191 Jun.
Kobell, F., 1834. Ueber den schillernden Asbest von Reichenstein in Schlesien. J. Prakt. Chem. 2, 297–298.
McClellan, R.O., Miller, F.J., Hesterberg, T.W., Warheit, D.B., Bunn, W.B., Kane, A.B., Lippmann, M., Mast, R.W., McConnell, E.E., Reinhardt, C.F., 1992. Approaches to evaluating the toxicity and carcinogenicity of man-made fibers: summary of a workshop held November 11-13, 1991, Durham, North Carolina. Regul. Toxicol. Pharmacol. 16 (3), 321–364 Dec.
McConnell, E.E., Davis, J.M., 2002. Quantification of fibrosis in the lungs of rats using a morphometric method. Inhal. Toxicol. 14 (3), 263–272 Mar.
McConnell, E.E., Axten, C., Hesterberg, T.W., Chevalier, J., Miiller, W.C., Everitt, J., Oberdörster, G., Chase, G.R., Thevenaz, P., Kotin, P., 1999. Studies on the inhalation toxicology of two fiberglasses and amosite asbestos in the Syrian golden hamster. Part II. Results of chronic exposure. Inhal. Toxicol. 11 (9), 785–835 Sep.
Moore, J.E., Bertram, C.D., 2018. 2018. Lymphatic system flows. Annu. Rev. Fluid Mech. 50, 459–482 Jan.
Oberdoerster, G., 1993. Lung dosimetry: pulmonary clearance of inhaled particles. Aerosol Sci. Technol. 18 (3), 279–289.
OECD 413, 2018. Test No. 413: Subchronic Inhalation Toxicity: 90-Day Study, OECD Guidelines for the Testing of Chemicals, Section 4, Health Effects. https://www.oecd-ilibrary.org/environment/test-no-413-subchronic-inhalation-toxicity-90-day-study_9789264070806-en.
Perkins, R.L., Harvey, B.W., 1993. Method for the Determination of Asbestos in Bulk Building Materials. EPA-600-R-93-116, July 1993. U.S. Environmental Protection Agency, Triangle Park, NC, USA.
Poland, C.A., 2019. Duffin R the toxicology of chrysotile-containing brake debris: implications for mesothelioma. Crit. Rev. Toxicol. 15, 1–25 Mar.
Pott, F., 1989. Carcinogenicity of fibers in experimental animals- data and evaluation. In: Mohr, U. (Ed.), Assessment of Inhalation Hazards. Springer-Verlag, Berlin Heidelberg, pp. 243–253.
Pott, F., Brown, R.C., 1991. Tumours by the Intraperitoneal and Intrapleural Routes and their Significance for the Classification of Mineral Fibres. Mechanisms in Fibre Carcinogenesis. Plenum Press, New York.
Riediker, M., Zink, D., Kreyling, W., Oberdörster, G., Elder, A., Graham, U., Lynch, I., Duschl, A., Ichihara, G., Ichihara, S., Kobayashi, T., Hisanaga, N., Umezawa, M., Cheng, T.J., Handy, R., Gulumian, M., Tinkle, S., Cassee, F., 2019. Particle toxicology and health - where are we? Part Fibre Toxicol. 16 (1), 19 Apr 23.
Rogers, R.A., 1999. In situ microscopic analysis of asbestos and synthetic vitreous fibers retained in hamster lungs following inhalation. Environmental Health Perspectives 107, 367–375.
Scallan, J.P., Zawieja, S.D., Castorena-Gonzalez, J.A., Davis, M.J., 2016. Lymphatic pumping: mechanics, mechanisms and malfunction. J. Physiol. 594 (20), 5749–5768 Oct 15.

Skinner, H.C.W., Ross, M., Frondel, C., 1988. Asbestos and Other FibrousMaterials — Mineralogy, Crystal Chemistry, and Health Effects. Oxford University Press, New York (NY).
Tanji, T., Yada, K., Akatsuka, Y., 1984. Alternation of clino- and orthochrysotile in a single fiber as revealed by high-resolution electron microscopy. Clay Clay Miner. 32 (5), 429–432.
Titulaer, M.K., van Miltenburg, J.C., Jansen, J.B.H., et al., 1993. Characterization of tubular chrysotile by thermoporometry, nitrogen sorption, drifts, and TEM. Clay Clay Miner. 41, 496–513.
Whittaker, E.J.W., 1957. The structure of chrysotile. V. Diffuse reflexions and fiber texture. Acta Crystallogr. 10, 149–156.
Whittaker, E.J.W., 1960. The crystal chemistry of the amphiboles. Acta Crystallogr. 13, 291–298.
Whittaker, E.J.W., 1963. Research report: Chrysotile fibers – filled or hollow tubes? Mathematical interpretation may resolve conflicting evidence. Chem Eng News 41, 34–35 September 30, 1963.
WHO, 1985. Reference methods for measuring airborne man-made mineral Fiber (MMMF). WHO/EURO MMMF Reference Scheme. Prepared by the WHO/EURO Technical Committee for Monitoring and Evaluating Airborne MMMF. World Health Organisation, Copenhagen.